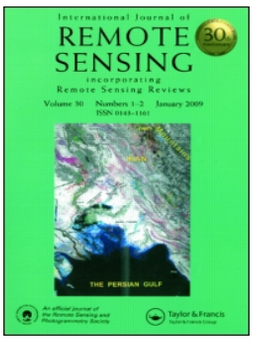

International Journal of Remote Sensing

ISSN: 0143-1161 (Print) 1366-5901 (Online) Journal homepage: https://www.tandfonline.com/loi/tres20

Spatial and temporal variations in vegetation coverage observed using AVHRR GIMMS and Terra MODIS data in the mainland of China

Yahai Zhang & Aizhong Ye

To cite this article: Yahai Zhang & Aizhong Ye (2020) Spatial and temporal variations in vegetation coverage observed using AVHRR GIMMS and Terra MODIS data in the mainland of China, International Journal of Remote Sensing, 41:11, 4238-4268, DOI: 10.1080/01431161.2020.1714781

To link to this article: https://doi.org/10.1080/01431161.2020.1714781

Published online: 03 Feb 2020.

INTERNATIONAL JOURNAL OF REMOTE SENSING
2020, VOL. 41, NO. 11, 4238–4268
https://doi.org/10.1080/01431161.2020.1714781

Taylor & Francis
Taylor & Francis Group

Spatial and temporal variations in vegetation coverage observed using AVHRR GIMMS and Terra MODIS data in the mainland of China

Yahai Zhang[a] and Aizhong Ye[a,b]

[a]State Key Laboratory of Earth Surface and Ecological Resources, Faculty of Geographical Science, Beijing Normal University, Beijing, China; [b]Key Laboratory of Soil Erosion and Prevention of Jiangxi Province, Jiangxi Institute of Soil and Water Conservation, Nanchang, China

ABSTRACT

Human activities and climate change have changed the vegetation in China. The analysis of the changes in vegetation that have occurred over the past 30 years in China remains a great challenge due to intense human activity and lack of field observations. The use of various Normalized Difference Vegetation Index (NDVI) datasets to study vegetation coverage changes has received much attention. In this paper, we selected the early versions of Advanced Very High Resolution Radiometer (AVHRR) Global Inventory Monitoring and Modelling Studies (GIMMS), GIMMS3g (third generation GIMMS NDVI from AVHRR sensors) and Moderate Resolution Imaging Spectroradiometer (MODIS) NDVI data including the fusion data (GIMMS+MODIS). We analysed spatial and temporal changes in vegetation cover in different ecosystems and basins in the mainland of China. Different contributions of ecosystems and variations in NDVI trends exist in different ecosystems in 17 basins. The results show that different NDVI from different data sources yield different results: (1) Vegetation increased in 74.62–77.7% of the area of the Chinese mainland during 1982–2015, mainly in the Yellow River and the middle reaches of the Yangtze River basin; (2) 2000–2017 MODIS NDVI in mainland China has increased more area (79.67%). (3) Farmland and Forest ecosystems were significantly enhanced in the eastern monsoon region; (4) High-resolution NDVI can provide more information than domain average NDVI. GIMMS and MODIS NDVI data have complementary spatial and temporal distributions. Our study improves the understanding of vegetation dynamics over long time periods and large areas and, moreover, has potential for supporting ecological managers in mainland China.

ARTICLE HISTORY
Received 29 July 2019
Accepted 26 November 2019

1. Introduction

In response to the challenges of unquestionable global climate change, the science of global change based on the overall behaviour of the earth system is rapidly developing (Bonan 2008; Lenzen et al. 2018; Li et al. 2018; Balato et al. 2008). As a major component of the terrestrial biosphere, vegetation is a key element of the global water and energy

CONTACT Aizhong Ye azye@bnu.edu.cn State Key Laboratory of Earth Surface and Ecological Resources, Faculty of Geographical Science, Beijing Normal University, Beijing 100875, China

cycles (Li et al. 2013; Guenther 2002; Jamali et al. 2015). Climate change can significantly affect vegetation activities and terrestrial carbon cycles (Gajewski 2015; Sarkar and Kafatos 2004; Yu et al. 2003). Monitoring the dynamics of regional or global vegetation cover and assessing the response of vegetation to global climate change are critical (Pan et al. 2018; Wang et al. 2018; Wu et al. 2015). With the continuous development of remote sensing technology, increasing amounts of satellite remote sensing data are provided, and the quality of data in, for example, resolution, precision, and noise reduction is improved. The technical improvements offer better support for global change studies (Dardel et al. 2014; Kaufman and Tanré 1996). Vegetation index is a simple and effective metric for surface vegetation coverage and growth status in the field of remote sensing. NDVI (Huete et al. 1997; Miura 2002), which is generated by remote sensing data, is the most widely used vegetation indices. NASA developed the Earth Resources Technology Satellite (ERTS), and became the pioneer of the Landsat satellite. Early sensors had minimal spectral resolution, tending to red and near-infrared bands (Tucker 1979), which is conducive for distinguishing between vegetation and clouds as well as other targets. (John and David, 2000) explain the meaning of NDVI and introduce it in terms of values. The NDVI is defined as near-infrared radiation (NIR) minus visible radiation (VIS) divided by the sum of near-infrared radiation and visible radiation. The range of NDVI values is from −1.0 to +1.0. The NDVI is linearly related to vegetation distribution density. Negative values indicate non-plant surfaces, whereas in areas with vegetation cover, NDVI increases with increasing vegetation coverage. Very low NDVI values (0.1 and below) correspond to barren areas of rock, sand, or snow. The median values represent shrubs and grasslands (0.2–0.3), while higher values represent temperate and tropical rainforests (0.6–0.8) (Myneni et al. 1995). Many researchers point out that NDVI is easily saturated in areas with high-vegetation coverage, and the value of NDVI no longer increases with the growth of vegetation, such as forests, cereals, and broad-leaved crops (Zhao, Liu, and Yang 2012; Gitelson, 2004; Le Maire et al. 2006; Ferrara et al. 2010). Because NDVI accurately reflects photosynthesis intensity and vegetation greenness, reflecting vegetation seasons and inter-annual variations, NDVI trends can be used as an indicator of greening or browning (Dardel et al. 2014; De Jong et al. 2011; Fensholt et al. 2009; Ju and Masek 2016). Therefore, NDVI has been widely used in global or continent-scale monitoring of vegetation dynamics (Jarlan et al. 2008; Tian et al. 2016), vegetation classification (Montandon and Small 2008; Wardlow, Egbert, and Kastens 2007), land cover change (Hill et al. 1999; Lunetta et al. 2006), phenology monitoring (Butt et al. 2011; Heumann et al. 2007), and so on.

The only AVHRR dataset with global coverage from the 1980s to the twenty-first century is GIMMS (Tucker et al. 2005). Global coverage of GIMMS data (GIMMS, 1981–2006) was released in 2007. After nearly 10 years, the GIMMS Study Group published the recently updated GIMMS3g NDVI dataset covering 1981–2015. MODIS NDVI processing (Huete et al. 2002) is a goal designed for vegetation monitoring, including the most advanced remote sensing technology. The technology reduces errors from the atmosphere, radiation, etc. and increase radiation sensitivity. Therefore, MODIS NDVI emerged as a powerful improvement in NDVI products derived from AVHRR sensors. MODIS NDVI data products began in 2000 and have been updated ever since. All of the above NDVI datasets are affected by time inconsistencies in trend analysis in different regions of the world (Gallo et al. 2004; Beck et al. 2011; Fensholt et al. 2012; Zhang et al. 2017) due to sensor differences and sensor transitions. At present, some conclusions from these studies

are recognized. For example, more consistency exists between GIMMS data and MODIS data on the temporal trends (Gallo et al. 2004). GIMMS3g data have strong consistency in time (Tian et al. 2015a), and the quality of AVHRR data is lower than the quality of the data collected by MODIS (Pettorelli et al. 2005), but GIMMS is a priority for long-term scale studies. Some studies have merged GIMMS and MODIS data, resulting in long-term sequence NDVI data, to explore long-term vegetation changes before GIMMS3g was released (Du et al. 2014; Mao et al. 2012a).

China is located in the eastern monsoon region of Asia, the climate of which is controlled mainly by the Westerlies. In addition, China has a diverse and distinct natural environment that covers almost all ecosystems from forest ecosystems to desert ecosystems with tropical to boreal vegetation. Thus, China is well suited and necessary for comparisons of different NDVI datasets. The previous study areas of vegetation change were mainly concentrated in arid and semi-arid areas, such as northern China (Dai, Zhang, and Wang 2010; Liu et al. 2010, 2017; Mao et al. 2012b; Song and Ma 2007; Sun 2012; Zhou et al. 2001), the Qinghai–Tibet Plateau (Wang and Han 2012; Xin, Xu, and Zheng 2008; Zhang et al. 2011), and the Loess Plateau (Jiang et al. 2015; Mao et al. 2012a; Xin, Xu, and Zheng 2008) in China. The arid and semi-arid areas are more sensitive regarding ecology or human activities. The overall vegetation increased in the 1980s and 1990s in China (Fang 2004; Piao 2003; Xiao and Moody 2004; Yun-hao et al. 2001). The SPOT VEGETATION NDVI and AVHRR GIMMS have good linearity in Chinese land surfaces (Song et al. 2010). The vegetation in China exhibited a significant increasing trend from 2001 to 2011 (Lin et al. 2013). There have been studies of vegetation changes over longer time series (Li et al. 2014; Peng et al. 2011; Piao et al. 2015; Xu et al. 2012), and it has been found that the trend has generally increased over the last three decades, especially in southern China. Scholars have realized that China's vegetation changes have staged trend characteristics (Liu et al. 2015; Peng et al. 2011; Piao et al. 2015), and then they choose their respective segmentation points to explore the changes in vegetation at different stages.

This study combined GIMMS and MODIS data into a set of fused data. Then compared GIMMS, GIMMS3g, MODIS and fused data in mainland China in order to reduce the uncertainty caused by multiple NDVI datasets. On this basis, it also evaluated the reliability of the fusion data fused by GIMMS and MODIS. We analysed the changes in vegetation cover in mainland China over the past three decades. Based on the policy of afforestation in China (Zhang et al. 2017), and the length of time of the NDVI datasets, we selected 2000 as a segmentation point for trend analysis. We have also explored the spatiotemporal agreement or disagreement of different NDVI datasets at multiple scales, including basin, ecosystem scales, and national scales.

2. Study area and data

2.1. Study area

The study area is the mainland of China, which excludes all coastal islands (Taiwan Island and islands such as the South China Sea Islands) except Hainan Island. China belongs to the East Asian monsoon region and is suffering from the adverse effects of climate change, like extreme weather, floods, typhoons, droughts, etc. In this study, China is divided into 17 hydrological and climatic regions (Figure 1, Table 1) according to watersheds. The

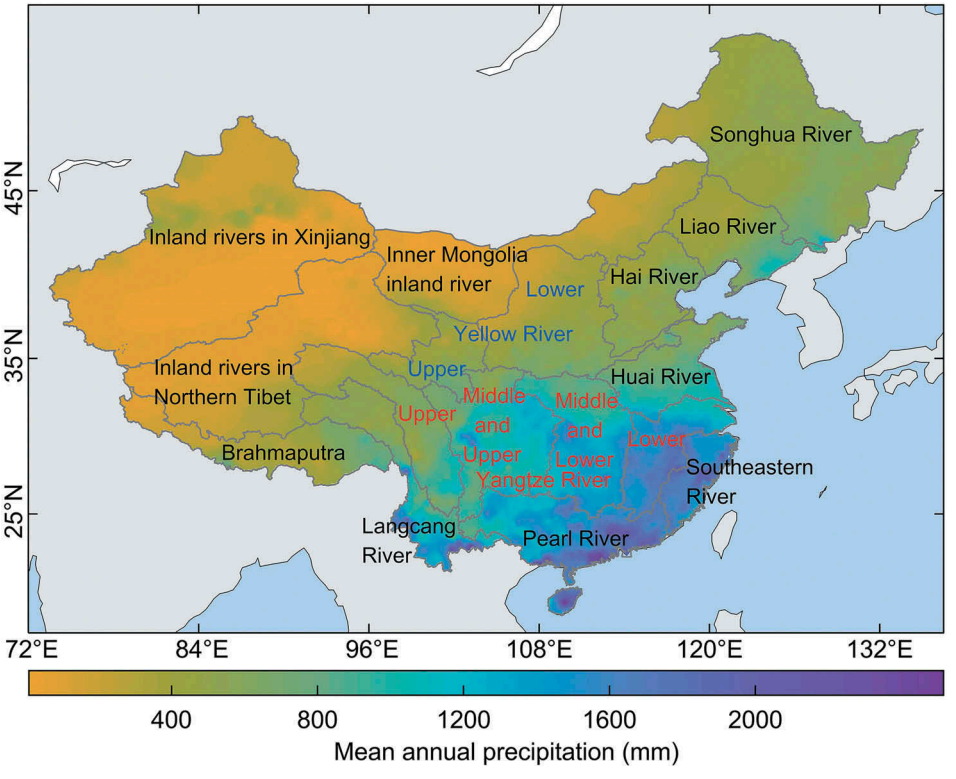

Figure 1. The 17 large hydro-climatic basins in mainland China and the distribution of mean annual precipitation (mm) in mainland China.

Table 1. Summary information of 17 river basins in China (Lang et al. 2014; Peel, Finlayson, and McMahon 2007).

Region	Full name	Mean annual precipitation (mm)	Area (km^2)
1	Songhua River	535.5	370,973
2	Liao River	566.1	310,117
3	Hai River	515.9	578,092
4	Inland rivers in Xinjiang	168.3	1,104,104
5	Lower Yellow River	391.0	448,864
6	Upper Yellow River	469.3	504,731
7	Lower Yangtze River	1606.5	324,061
8	Huai River	819.5	415,287
9	Inland rivers in Northern Tibet	199.9	694,413
10	Southeastern River	1705.9	226,496
11	Brahmaputra	876.7	908,881
12	Upper Yangtze River	795.2	399,541
13	Middle and Lower Yangtze River	1276.5	567,237
14	Middle and Upper Yangtze River	1001.1	323,970
15	Pearl River	1700.7	567,520
16	Lancang River	882.2	316,057
17	Inner Mongolia inland river	220.4	1,537,520

classification of climate types in these regions, such as the Koppen–Geiger climate type (Peel, Finlayson, and McMahon 2007), attempts to ensure that regional climate has nearly uniform characteristics when zoning. In this paper, 17 hydro-climatic basins are abbreviated as basins.

In 17 basins, Inner Mongolia inland river has the largest area of 1,537,520 km^2 with cold semiarid climate and the climate type of Lower Yellow River (448,864 km^2) is the same with it. Southeastern River has the smallest area of 226 496 km^2, and the climate type is warm oceanic climate or humid subtropical climate. In general, the largest climate type in China is the temperate-continental climate.

2.2. Data

2.2.1. NDVI datasets

MODIS NDVI, GIMMS NDVI, and GIMMS3g NDVI were selected in this paper. GIMMS NDVI dataset is the global vegetation index change dataset launched by the National Aeronautics and Space Administration (NASA). The dataset includes global NDVI data computed from the red and near-infrared bands from July 1981 to December 2006 (Tucker et al. 2005) and with a time resolution of half a month, spatial resolution of 8 km, and Albers-Conic-Equal-Area projection. The GIMMS NDVI dataset was calibrated by sensors, including NOAA (national oceanic and atmospheric administration) −7, NOAA-9, NOAA-11 sensors (1981–1999), NOAA-14 sensors (January 1995–November 2000), NOAA-16 (2000) (November 2000 to December 2003), and NOAA-17 (December). It also improves the sensor sensitivity to the spectrum and discontinuous changes over time, corrects for radiation, clouds, the atmosphere, and solar elevation angle (Tucker et al. 2005), and uses EMD (Empirical Mode Decomposition) to mitigate the drift of satellite orbits. The GIMMS NDVI archive is considered to be the best dataset available for long-term NDVI trend analysis (Beck et al. 2011).

The third generation GIMMS AVHRR is the longest-term global vegetation index product, and has become an important source of data for studying large-scale ecological processes (Liu et al. 2017; Pan et al. 2018; Pinzon and Tucker 2014; Wang et al. 2017). GIMMS3g dataset time series has been extended for nearly 35 years (1982–2015). Since the data has been pre-processed, the accuracy is effectively improved, and the data quality and spatiotemporal resolution are exceptional. (Pinzon and Tucker 2014). The data offer a good chance for investigating long-term vegetation cover changes.

The Global MODIS NDVI (Huete et al. 2002) is designed to provide spatial and temporal information of vegetation conditions. The 1-km spatial resolution MOD13A3 products from 2000 to 2017 for the mainland of China were obtained from the NASA Reverb website (http://reverb.echo.nasa.gov/). NDVI images were directly derived from the MOD13A3 products, which provides a 3-level sinusoidal projection grid product. During the processing of monthly products, the algorithm absorbs all 1 km of products covering the entire month for 16 days. If there is no cloud in the atmosphere, the time-weighted average method is adopted, or the minimum value is adopted to prevent clouding influence. On the basis of 1B data, the product corrects the edge distortion caused by the remote sensor imaging process. The MODIS Vegetation Index product V5 has been confirmed in the third phase (Adami et al. 2018; Sun et al. 2015; Solano et al. 2010).

2.2.2. China's terrestrial ecosystems

The macro-structure data of 2015 China's terrestrial ecosystems were used in this study, and we downloaded that data from the Resource and Environmental Science Data Center of the Chinese Academy of Sciences (http://www.resdc.cn/). The 1:100,000-scale land use/

land cover data were obtained by remote sensing interpretation. The macro-structure data of 2015 China's terrestrial ecosystems is one of the ChinaEco100-Spatiotemporal Distribution Dataset of Ecosystem Types in China. ChinaEco100-Spatiotemporal Distribution Dataset of Ecosystem Types in China is based on Landsat TM/ETM/OLI remote sensing imagery. After image fusion, geometric correction, image enhancement, and splicing, it is interpreted by human-computer interaction (Xu et al. 2017). The spatial resolution of the dataset is 100 metres. Based on the identification and research of various ecosystem types, the spatial distribution data sets of multi-period China terrestrial ecosystem types are formed through classification. This dataset divides China's land into seven major ecosystem types, including farmland ecosystems, forest ecosystems, grassland ecosystems, water and wetland ecosystems, desert ecosystems, settlement ecosystems, and other ecosystems (Figure 2).

To further explore the contribution or change of ecosystems in each basin and gather statistics on the trends of ecosystems, this study attempted to discover the trends of different NDVI datasets in ecosystems of each unit. The proportions of different ecosystems in the 17 basins are obviously varied (Figure 3). From east to west, the dominant ecosystem changes from forest ecosystem and farmland ecosystem to grassland ecosystem and desert ecosystem. The greater the proportion of the ecosystem, the greater the contribution to vegetation changes reflecting the NDVI trend of the basins. The farmland ecosystem is the main ecosystem of Liao River, Huai River, Hai River, and the Lower Yellow River, while Songhua River, Southeastern River, Pearl River, and Yangtze River (except

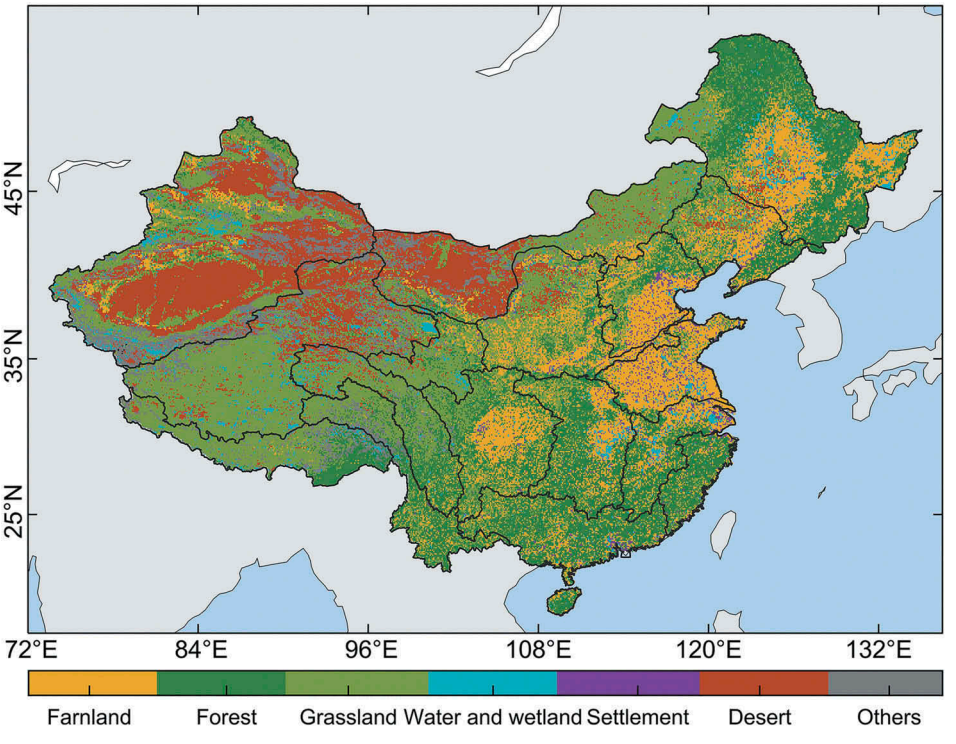

Figure 2. The terrestrial ecosystem types of China.

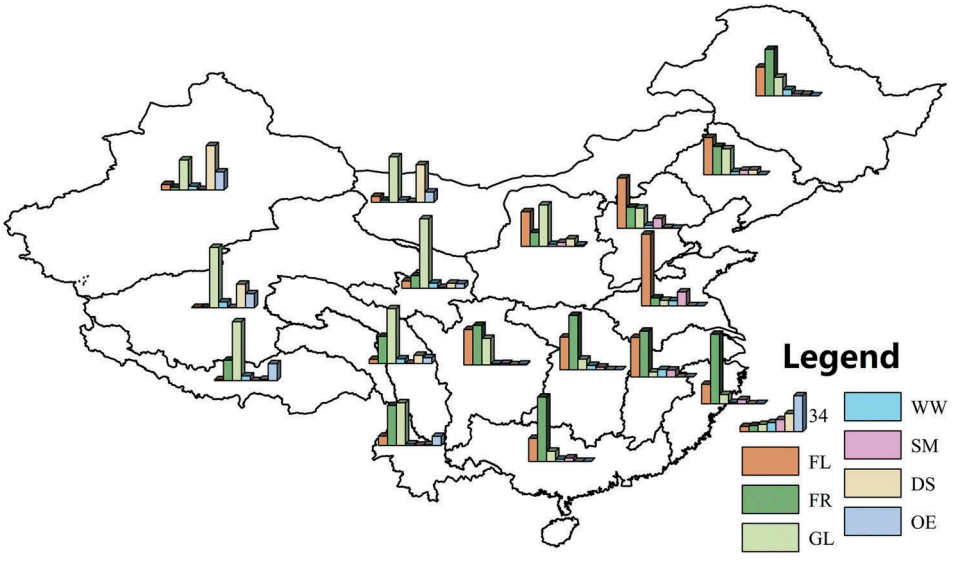

Figure 3. The percentage of ecosystems in 17 basins. The abbreviations in the legend represent the different ecosystems. FL: Farmland; FR: Forest; GL: Grassland; WW: Water and Wetland; SM: Settlement; DE: Desert; OE: Others. Each bar represents the proportion of each ecosystem in this basin, and the sum of each bar in one basin is 100%. The number 34 of legend means the value of the histogram with the height closest to the number.

Upper Yangtze River) are dominated by forest ecosystems. Grassland ecosystems account for a large proportion in Inner Mongolia inland river, Upper Yellow River, Upper Yangtze River, Inland rivers in Xinjiang, Inland rivers in Northern Tibet and Brahmaputra.

2.2.3. Other data

The gridded daily precipitation and temperature observations for 1982–2015 at a 0.5-degree resolution were obtained from the National Meteorological Information Center, CMA (http://data.cma.cn/). The information of rural population dataset was from 1982–2015 China Statistical Yearbook, and the 1982–2015 afforestation area was downloaded from China Forestry Yearbook. The specific information can be seen in Table 2.

3. Data post-processing and methodology

3.1. Data post-processing

By using the maximum-value composite technique (Holben 2007), 15-day GIMMS NDVI and GIMMS3g NDVI were aggregated to monthly temporal resolution. We also applied the same method to GIMMS3g and got monthly GIMMS3g NDVI data. For the purpose of consistency, the MODIS dataset was resampled to the same spatial resolution of GIMMS (8 km), as well as making projection transformation before analysis. NDVI values lower than 0.1 were set to 0.1, which is equivalent to shielding those areas so as not to affect the detection and to better reflect the changes in vegetation coverage.

In this study, we consider the area where NDVI is greater than 0.6 to be the high-value area of NDVI, and the area below 0.3 is considered to be the low-value area of NDVI.

Table 2. Information of other data for the mainland China.

Data type	Spatial resolution	Temporal resolution	Time period	Source
Precipitation	0.5 ° (≈55km)	Daily	1982 ~ 2015	CMA (http://data.cma.cn/)
Temperature	0.5 ° (≈55km)	Daily	1982 ~ 2015	
The proportion of Rural Population	-	Yearly	1982 ~ 2015	China Statistical Yearbook
The afforestation area	-	Yearly	1982–2015	China Forestry Yearbook

' – ' means no data.

Because of the saturation of NDVI, we set 0.8 as the upper threshold of NDVI. Since the two sets of data are different in many non-ignorable aspects, such as satellite sensors, spatial resolution, temporal resolution, etc. The two datasets need to be pre-processed before the two sets of data are fused. To obtain the long-term NDVI composite data composed of monthly GIMMS and MODIS NDVI, the correlation analysis of the two datasets had to be checked first. The Pearson correlation coefficient can be expressed as follows:

$$r = \frac{\mathrm{cov}(x, y)}{\sqrt{\mathrm{var}(x)\mathrm{var}(y)}} \tag{1}$$

where the r value is the correlation, x and y are the 2000–2006 monthly average GIMMS and MODIS NDVI values, cov is the covariance between x and y, and var is the variance function.

The distribution of correlation coefficients between them is shown in Figure 4. There are 80.90% of the pixels having a correlation coefficient greater than 0.7. Therefore, GIMMS and MODIS have a high correlation and meet the requirements of integration.

Linear regression at the per-pixel level was then applied to monthly MODIS NDVI and GIMMS NDVI (2000–2006) data. Next, using this regression equation, a new MODIS for 2000–2015 is obtained, which is connected with GIMMS before 2000. The new 2000–2015 NDVI data were prolonged through the pixel-by-pixel linear regression equations. Then, all the NDVI datasets were averaged over the whole study area. The per-pixel linear regression model can be applied to every pixel, leading to the most accurate regression equation (Montgomery, Peck, and Vining 2012). The applied formulas are as follows:

$$G_i = a + b \times M_i + \varepsilon_i \tag{2}$$

$$b = \frac{n\sum_{i=1}^{n} M_i G_i - \sum_{i=1}^{n} M_i \sum_{i=1}^{n} G_i}{n\sum_{i=1}^{n} M_i^2 - \left(\sum_{i=1}^{n} M_i\right)^2} \tag{3}$$

$$a = \bar{G} - b \times \bar{M} \tag{4}$$

Parameters in the model are calculated by the least squares. ε_i refers to a random error. M_i and G_i represent separately MODIS NDVI and GIMMS NDVI matching the i-th months. n is the total number of months. $\bar{G}$ is the mean of 2000–2006 monthly GIMMS data for the corresponding pixels. $\bar{M}$ represents values under the same conditions for MODIS. In this way, this new long-time NDVI data can be constructed and prepared for further research.

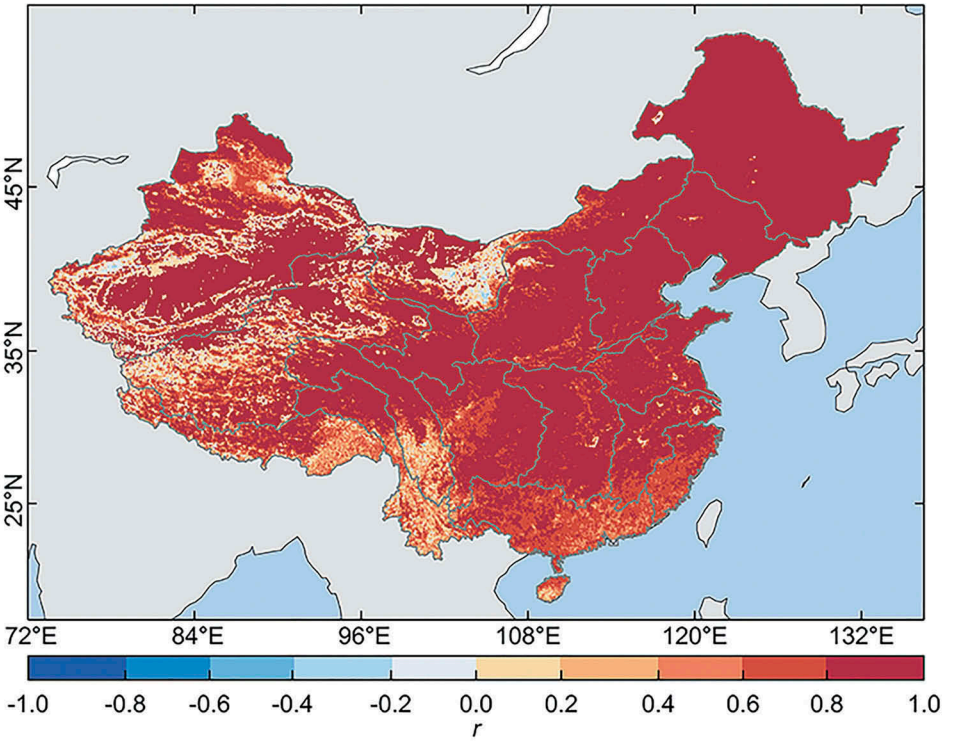

Figure 4. The correlation between MODIS NDVI and GIMMS NDVI.

3.2. Linear regression

The linear regression method was used to establish GIMMS and MODIS regression equations for data post-processing (Section 3.1) and also obtains the trend term of NDVI in the mainland of China, which was used for indicating the inter-annual variation of vegetation at the pixel level.

In this study, year is defined as an independent variable, the annual average NDVI value is defined as the dependent variable, and the least squares method is used to optimize the slope by minimizing the sum of the squared errors. When the slope is positive, it indicates that the vegetation cover increases or the improving vegetation trend; conversely, when the slope is negative, it means that the vegetation cover decreases and the vegetation dynamic change shows a downward trend.

The slope of the fitting function can be expressed as follows:

$$\text{Slope} = \frac{k\sum_{j=1}^{k} j \times \text{NDVI}_j - \sum_{j=1}^{k} j \sum_{j=1}^{k} \text{NDVI}_j}{k\sum_{j=1}^{k} j^2 - \left(\sum_{j=1}^{k} j\right)^2} \tag{5}$$

where the Slope represents the trend in the NDVI time series, k represents the cumulative number of years in every period, j represents the number of the year (j = 1,2,3, …, k), and NDVI represents the NDVI value corresponding to the j-th year.

3.3. Mann-Kendall test

The Mann-Kendall (M-K) nonparametric statistical method (Mann 1945; Kendall 1975) is currently widely used in trend analysis (de Beurs et al. 2004; Zhang et al. 2016; Pouliot, Latifovic, and Olthof 2009; Neeti et al. 2011). It can effectively distinguish whether a process is in natural fluctuation or has a definite trend of change. Its advantage is that it does not require samples to follow a certain distribution and is not affected by a few outliers. The calculation method is as follows.

The statistic S is calculated using Eqs. (6–8).

$$S = \sum_{l=1}^{m-1} \sum_{q=l+1}^{m} \operatorname{sgn}(x_q - x_l) \tag{6}$$

$$\operatorname{sgn}(x_q - x_l) = \begin{cases} 1 & (x_q - x_l) > 0 \\ 0 & (x_q - x_l) = 0 \\ -1 & (x_q - x_l) < 0 \end{cases} \tag{7}$$

$$\mathrm{E}(S) = 0 \quad \operatorname{var}(S) \approx \frac{m(m-1)(2m+5)}{18} \tag{8}$$

where $\{x_1, x_2, \cdots, x_m\}$ is the time-series data, sgn () is a symbolic function, and m is the number of data points. E (S), var (S) are the mean and variance of the statistic S, respectively. When m > 10, the standard normal test statistic Z is computed using Eq. (9).

$$Z = \begin{cases} \frac{S-1}{\sqrt{\operatorname{var}(S)}} & S > 0 \\ 0 & S = 0 \\ \frac{S+1}{\sqrt{\operatorname{var}(S)}} & S < 0 \end{cases} \tag{9}$$

The M-K statistic Z-value of the calculated time series is used to test the significance of trend statistics. Z-value has a range of (-∞, +∞). A positive Z-value indicates that the time series (Zhang et al. 2017) has an upward trend, while a negative Z-value indicates a downward trend. $|Z| > Z_{0.05/2} = 1.96$, indicating that the sequence trend changes significantly.

In the trend analysis, 2000 was picked as our segmentation point. Over-exploitation of forests in China for more than 50 years has led to serious ecological degradation at the end of the twentieth century, including soil erosion, desertification, sandstorms, and flooding, especially the 1998 floods. In response to the damage caused by these disasters and the serious consequences of the 1998 floods, the Chinese government has taken many important measures since 1998 to implement sustainable forest management (SFM) in China (Dai et al. 2011). In 2000 and 2001, the Chinese government established the 'Six Major Forestry Projects' to control soil erosion, reduce floods, protect biodiversity, and restore degraded ecosystems (Xu et al. 2018). Since the vegetation restoration project has been widely implemented, the vegetation situation in China has undergone changes. We

considered choosing a segmentation point in the interval from the end of the twentieth century to the beginning of the twenty-first century. On the other hand, the MODIS data started from 2000. In order to better compare different NDVI datasets and can scan the change process of MODIS NDVI data from the beginning, we chose 2000 as a segmentation point for this analysis of vegetation cover change in mainland China.

4. Results

4.1. Annual average of NDVI distribution spatial pattern

Figure 5 shows the distributions of the annual average NDVI of the three NDVI datasets over different periods. It can be concluded that there has been no significant change in the distribution pattern of high and low NDVI value areas in China during the past nearly four decades. The three sets of NDVI data give similar results, although the magnitudes of the values differ.

The NDVI in mainland China presents a low-value spatial distribution pattern in the northeast, southeast, southwest, and northwest basins. A relatively clear boundary line is approximately formed at the 400 mm precipitation line in China. The high-vegetation coverage in Southeast China and the low-vegetation coverage in Northwest China were confirmed on the NDVI maps. China's 400 mm precipitation line is also the boundary between semi-humid and semi-arid regions, forests, and grasslands in China. The distribution map of China's vegetation index correlates with the distribution of atmospheric precipitation (Figure 1). In areas with high-vegetation density, the NDVI values of GIMMS3g are higher and more obvious than GIMMS and MODIS data. The difference between high and low GIMMS3g NDVI values is obvious. GIMMS3g can better identify areas with higher NDVI values.

In Figure 6, there are more consistent and few changes with time in Inland rivers in Xinjiang, Inland rivers in Northern Tibet, and Inner Mongolia inland river which are regions with sparse vegetation coverage. Comparing the 1982–2015 GIMMS+MODIS and 1982–2015 GIMMS3g (Figure 6(a)), the two datasets have little difference in the range of the (0.1,0.3], but the difference in the (0.6,1] is larger, and the proportion of GIMMS3g is significantly more than GIMMS+MODIS. From Figure 6(b), 1982–2000 GIMMS3g NDVI of the range of (0.6,1] in Songhua River, Yangtze River, and Huai River is obviously higher than GIMMS in the same period. The (0.1,0.3] proportion of GIMMS3g in 2000–2015 is lower than that in 1982–2000, and the proportion of high-value area is higher. The area without vegetation cover has decreased except for Inland rivers in Xinjiang. The proportion of Huai River in the (0.6,1] increased the most (Figure 6(c)). The percentage of (0.6,1] of GIMMS3g is larger than that of MODIS (Figure 6(d)). The proportions of each NDVI interval in 2000–2015 and 2000–2017 MODIS have not changed much (Figure 6(e)). The (0.6,1] is the interval where the contribution of the increase is relatively large, which is reflected in the Songhua River, Lower Yellow River, Hai River, and Liao River.

4.2. Trend analysis of NDVI in mainland China

Figure 7 shows that the variations in general trend changes (regression slope values) in different NDVI datasets are quite similar overall but not partially. The GIMMS+MODIS NDVI

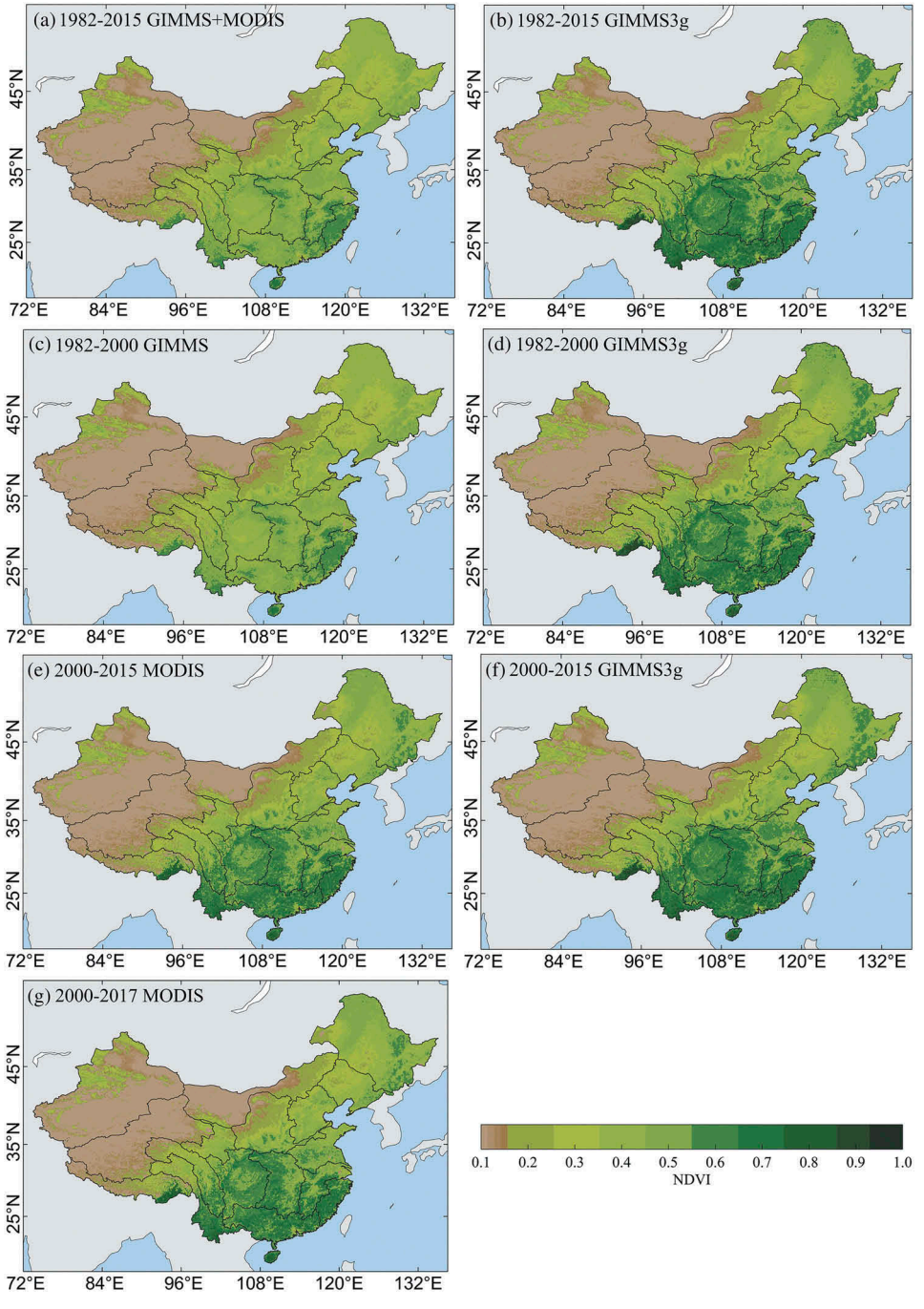

Figure 5. Annual averages of the different NDVI datasets in mainland China.

(Figure 7(a)) increased, and the GIMMS3g NDVI (Figure 7(b)) decreased in the Songhua River Basin during 1982–2015. That is to say, GIMMS+MODIS NDVI shows revegetation, and GIMMS3g NDVI shows deterioration in the Songhua River Basin. The variation between the GIMMS (Figure 7(c)) and GIMMS3g (Figure 7(d)) NDVI trends were more

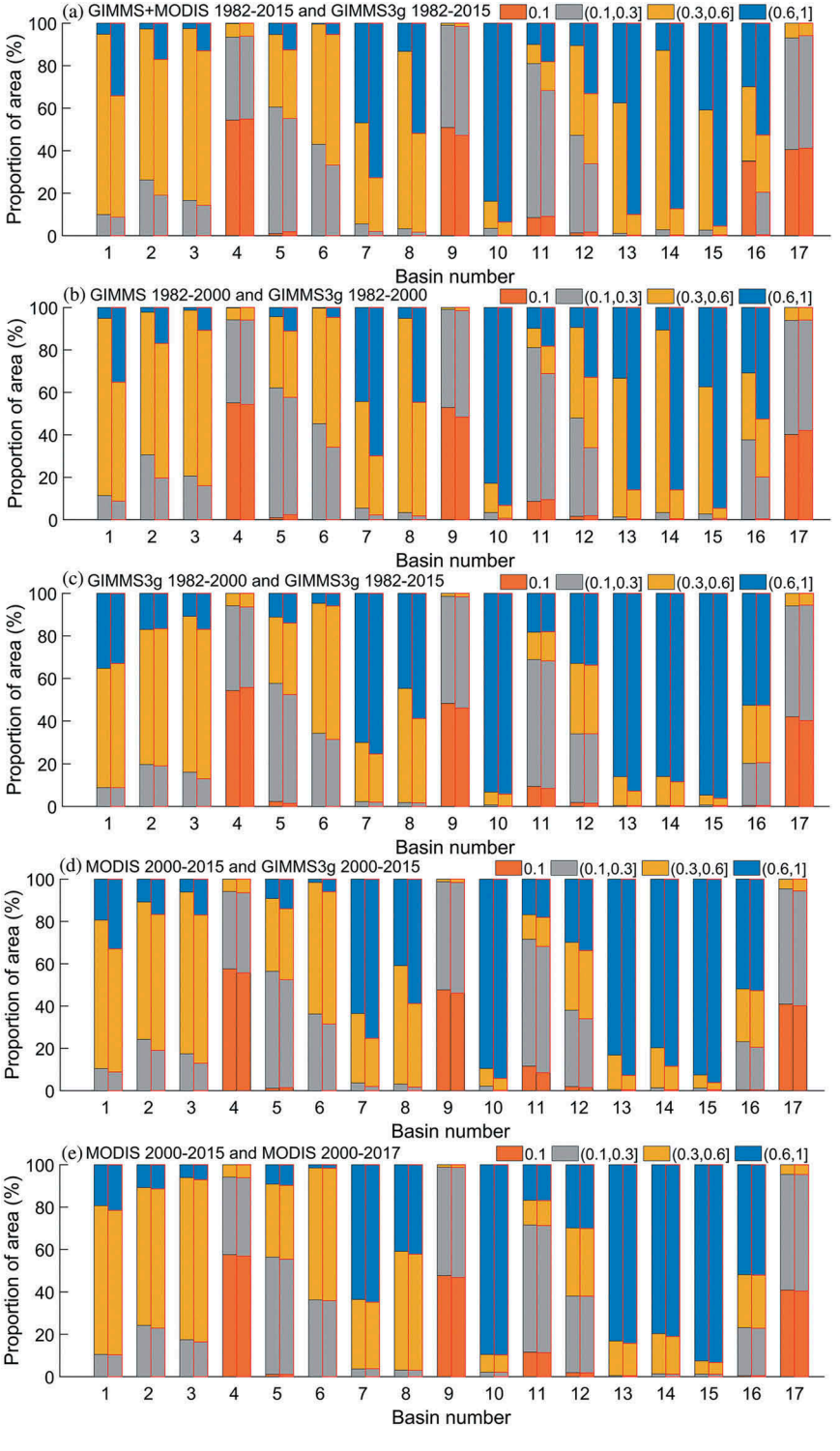
(a) GIMMS+MODIS 1982-2015 and GIMMS3g 1982-2015
(b) GIMMS 1982-2000 and GIMMS3g 1982-2000
(c) GIMMS3g 1982-2000 and GIMMS3g 1982-2015
(d) MODIS 2000-2015 and GIMMS3g 2000-2015
(e) MODIS 2000-2015 and MODIS 2000-2017
0.1
(0.1,0.3]
(0.3,0.6]
(0.6,1]
Proportion of area (%)
Basin number

distinct in the basins of the Huai River, Pearl River, Lower Yangtze River, and Southeast River during 1982–2000. The vegetation change trends were obviously opposite between MODIS (Figure 7(e)) and GIMMS3g NDVI (Figure 7(f)) during 2000–2015 in the Songhua River Basin and the southwestern basins (including Lancang River, Upper Yangtze River, and Brahmaputra). There is an increasing trend in vegetation in Songhua River and the southwestern basins during 2000–2015 (Figure 7(e)). While in these regions, there is a noticeable deterioration, overall (Figure 7(f)).

Comparing the spatial distributions of the MODIS NDVI slopes during 2000–2015 (Figure 7(e)) and 2000–2017 (Figure 7(g)), the slopes during 2000–2017 are bigger than the slopes during 2000–2015. MODIS 2000–2017 is significantly greener than MODIS 200–2015 in Pearl River, Yangtze River (except Upper Yangtze River), Lower Yellow River as well as the northern part of Songhua River. The results show rapid revegetation during 2015–2017.

The frequency distributions (Figure 8) of the three NDVI data sets' slopes are relatively consistent, and most of the pixel values are concentrated between -2×10^{-3} and 2×10^{-3} per year. Concerning the slopes, 63.74%-68.49% of them are greater than zero, showing that vegetation increased in 63.74%-68.49% of the area of mainland China during 1982–2015 (Figure 8(a)). GIMMS3g NDVI slopes show that vegetation increased in 73.93% of the area of mainland China during 1982–2000 (Figure 8(b)) and 57.23% of the area of China during 2000–2015 (Figure 8(c)). However, MODIS NDVI slopes show that vegetation increased in 75.03% of the area of mainland China during 2000–2015 (Figure 8(c)) and 79.67% of the area during 2000–2017 (Figure 8(d)). Recent MODIS products are considered to have good sensor calibration and high spatial resolution (Fensholt et al. 2009; Fensholt and Proud 2012). We combined the trend of GIMMS and GIMMS3g before 2000 and MODIS data after 2000. Therefore, we confirm that vegetation increased to more than 70% of the area of China during 1982–2017.

The significant trends of NDVI in different stages (M-K statistic *Z*-values) as derived from MODIS, GIMMS, and GIMMS3g data are shown in Figure 9. A general increase in vegetation is more significant and similar from GIMMS+MODIS NDVI (Figure 9(a)) and GIMMS3g (Figure 9(b)) in mainland China during 1982–2015, except in the Songhua River Basin. The prominent revegetation areas are in the Yellow River and the Huai River Basins. The deterioration of vegetation areas is found mainly in the eastern Songhua River, the

Figure 6. The proportion of four NDVI value intervals in 17 basins under different data sources. The names of the 17 basins correspond to the number codes referred to in Table1: 1: Songhua River; 2: Liao River; 3: Hai River; 4: Inland rivers in Xinjiang; 5: Lower Yellow River; 6: Upper Yellow River; 7: Lower Yangtze River; 8: Huai River; 9: Inland rivers in Northern Tibet; 10: Southeastern River; 11: Brahmaputra; 12: Upper Yangtze River; 13: Middle and Lower Yangtze River; 14: Middle and Upper Yangtze River; 15: Pearl River; 16: Lancang River; 17: Inner Mongolia inland river. The '0.1' means that a value less than 0.1 is set to 0.1, indicating that there is no vegetation coverage. (a) the comparison between 1982–2015 GIMMS+MODIS and 1982–2015 GIMMS3g, columns with red wireframes represent 1982–2015 GIMMS3g. (b) the comparison between 1982–2000 GIMMS and 1982–2000 GIMMS3g, columns with red wireframes represent 1982–2000 GIMMS3g. (c) the comparison between 1982–2000 GIMMS3g and 2000–2015 GIMMS3g, columns with red wireframes represent 2000–2015 GIMMS3g. (d) the comparison between 2000–2015 GIMMS3g and 2000–2015 MODIS, columns with red wireframes represent 2000–2015 MODIS. (e) the comparison between 2000–2015 MODIS and 2000–2017 MODIS, columns with red wireframes represent 2000–2017 MODIS.

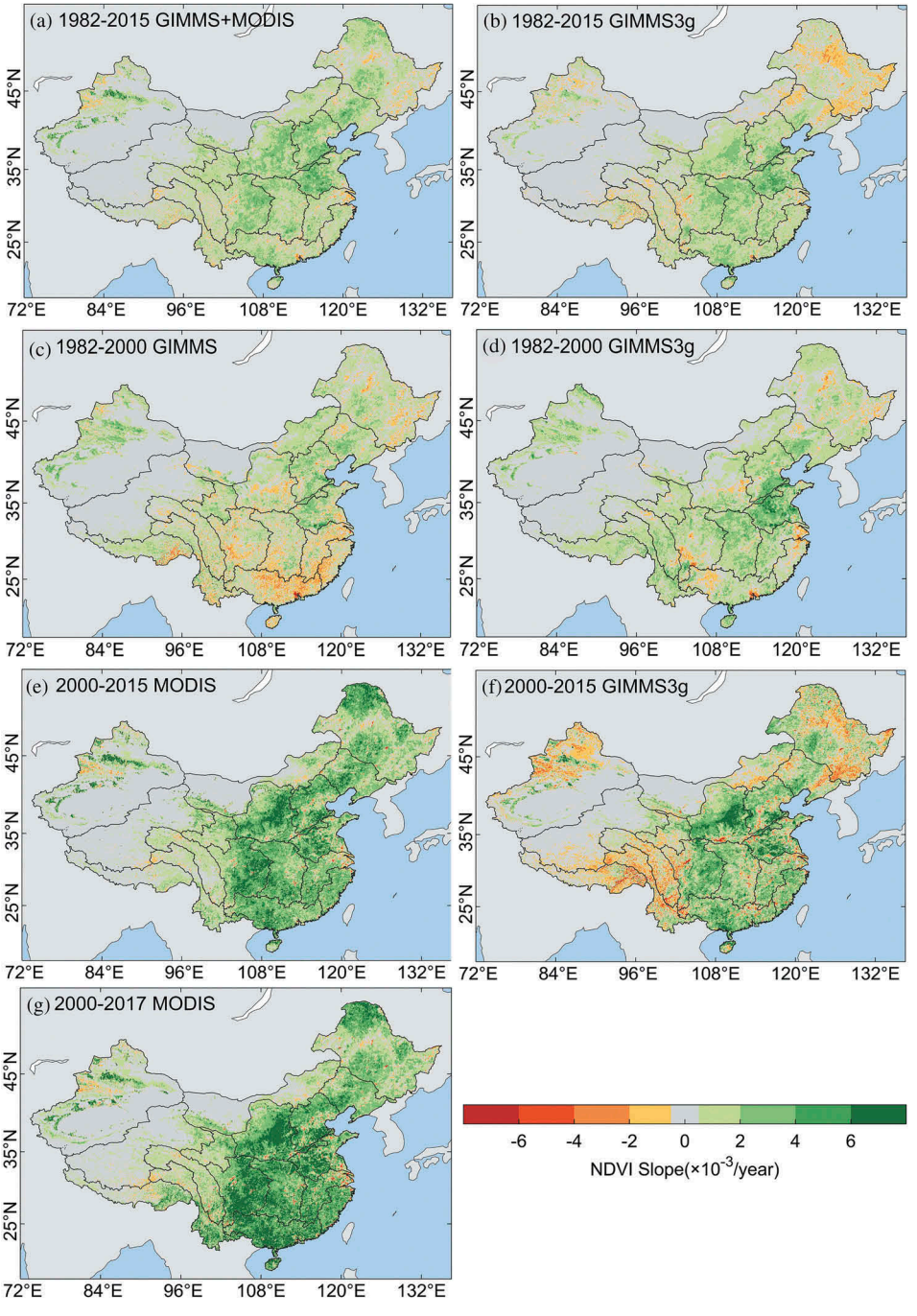

Figure 7. Slope in NDVI for mainland China, 1982–2017.

Xinjiang northern part, and the southwest regions, including the Pearl River Delta and Yangtze River Delta regions. GIMMS *Z*-values (Figure 9(c)) show more partial negative trends than GIMMS3g *Z*-values (Figure 9(d)) during 1982–2000 in south China. GIMMS can

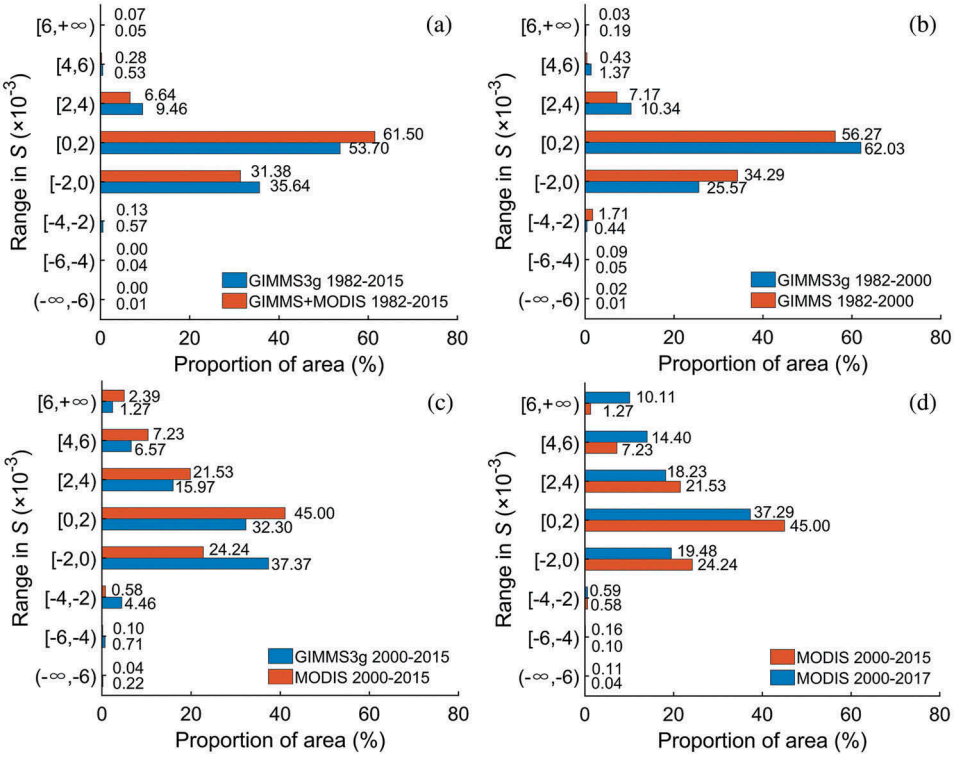

Figure 8. The frequency distributions of NDVI changed slopes at different times; *S* represents the Slope. (a) GIMMS+MODIS and GIMMS3g 1982–2015; (b) GIMMS and GIMMS3g 1982–2000; (c) MODIS and GIMMS3g 2000–2015; (d) MODIS 2000–2015 and MODIS 2000–2017.

underestimate the greening trend of vegetation. Most of the MODIS *Z*-values (Figure 9(e)) are positive, showing upward trends of vegetation during 2000–2015. However, the GIMMS3g *Z*-values (Figure 9(f)) show downward trends of vegetation in the southwest, northwest, and northeast. We added MODIS NDVI data during 2016–2017 and found that the upward trends of vegetation are more significant (Figure 9(g)).

Figure 10 presents the frequency distributions of M-K *Z*-value for different times. The vegetation increased ($Z > 0$) in 74.62%-77.7% of the area of China's mainland during 1982–2015 from the GIMMS+MODIS and GIMMS3g *Z*-values frequency distributions (Figure 10(a)). This result deviates from the result of the slope (63.74%-68.49%), which we believe is the bias caused by the different methods. Both methods can reflect the trend of NDVI change so that they can confirm each other. The vegetation increased ($Z > 1.96$) significantly in 41.54%-47.73% of the area of the Chinese mainland during 1982–2015. GIMMS+MODIS has 6.19% more area with *Z*- values greater than 1.96 then GIMMS3g. GIMMS+MODIS shows a larger area of revegetation. The vegetation decreased remarkably ($Z < -1.96$) in 6.21%-8.61% of the area of China's mainland during 1982–2015. The proportion of vegetation degradation is less than 10%, which we believe is within the controllable range. The vegetation increased ($Z > 0$) in 85.99% of the area of China's mainland during 1982–2000 from GIMMS3g, which is greater than for GIMMS (71.45%) (Figure 10(b)). However, the vegetation increased ($Z > 0$) in 69.55% of the area of China's mainland during

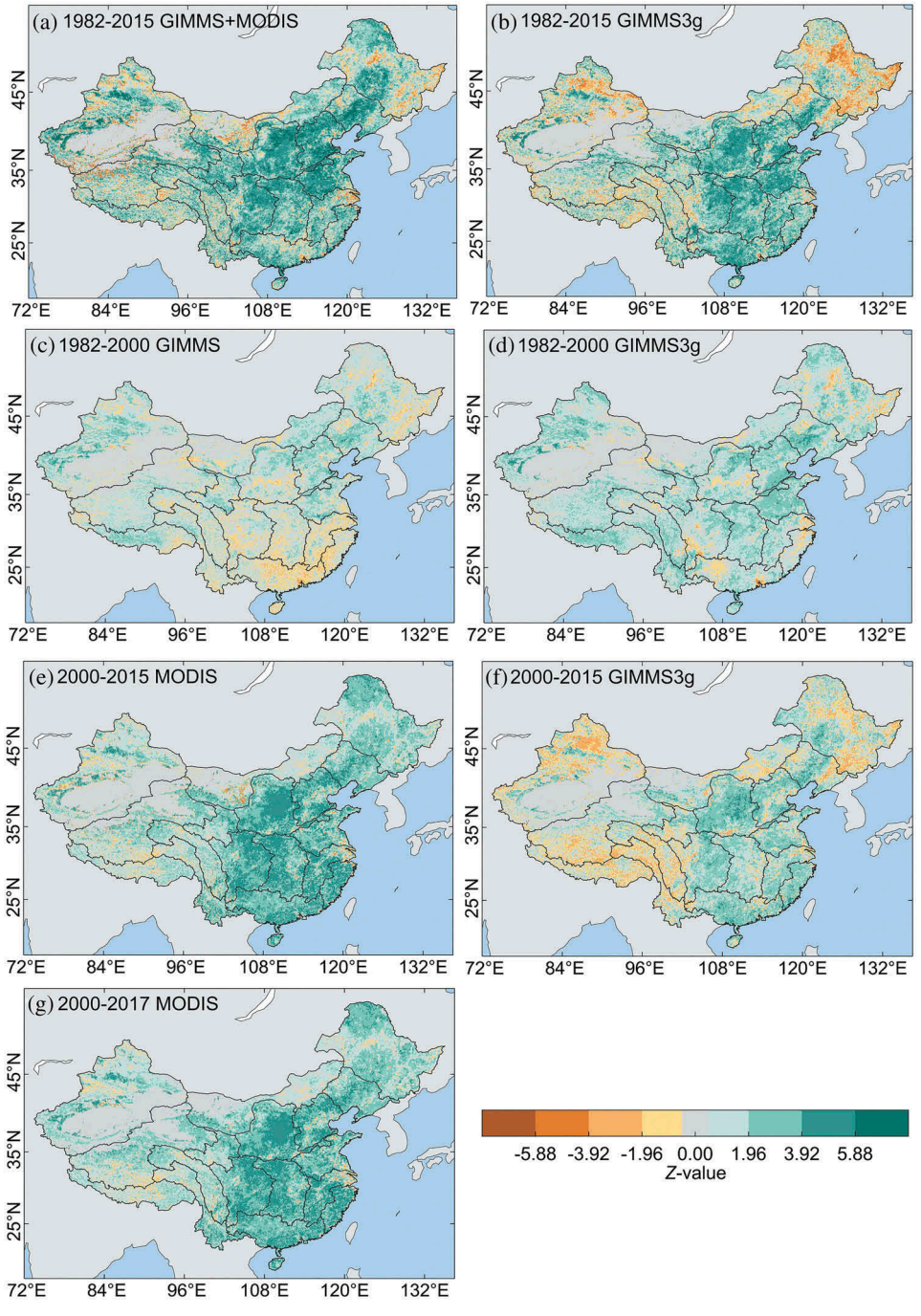

Figure 9. The M-K *Z*-value of the NDVI variations in mainland China.

2000–2015 from GIMMS3g, which is less than for MODIS (87.52%) (Figure 10(c)). From 1982 to 2000, the proportion of vegetation increased significantly ($Z > 1.96$) from 13.60% to 25.04%. Compared with it, the proportion of 2000–2015 vegetation increased significantly

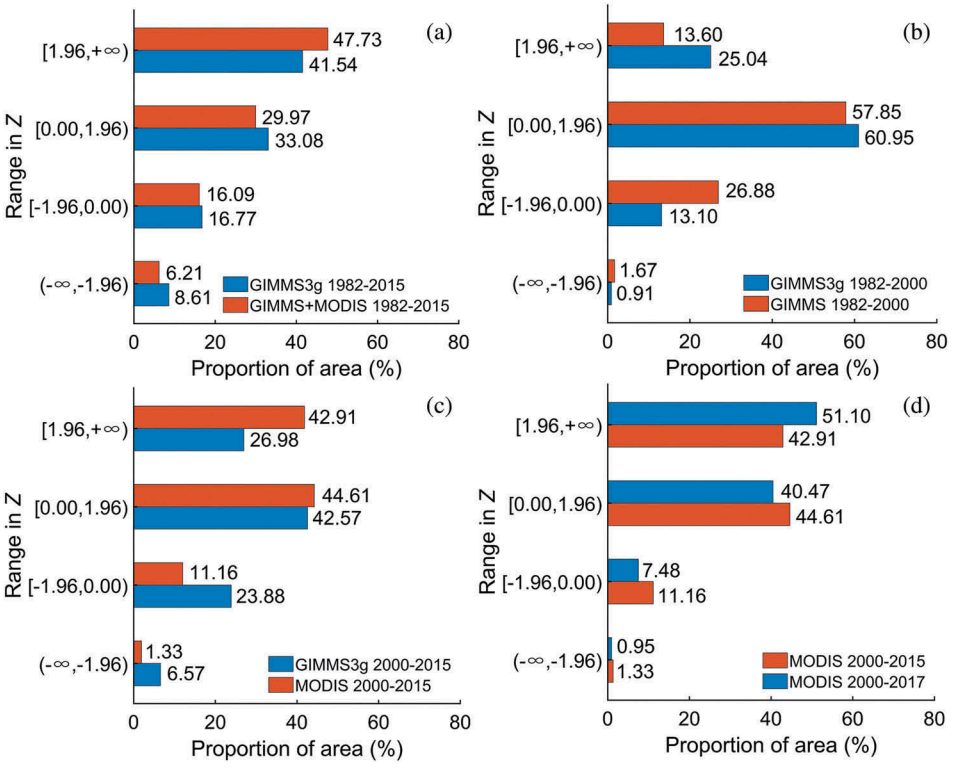

Figure 10. The frequency distributions of M-K *Z*-value at different times. (a) GIMMS+MODIS and GIMMS3g 1982–2015; (b) GIMMS and GIMMS3g 1982–2000; (c) MODIS and GIMMS3g 2000–2015; (d) MODIS 2000–2015 and MODIS 2000–2017.

from 26.98% to 42.91%, and it increased by 13.38%-17.87%. The vegetation increased ($Z > 0$) in 91.57% of the area of China's mainland during 2000–2017 from MODIS (Figure 10(d)), and the vegetation increased rapidly during 2016–2017.

The results of the Mann-Kendall nonparametric test are similar to those of the linear regression trend analysis; Mann-Kendall test can not only verify the significance but also provide evidence of a trend change, eliminating the uncertainty of the analytical method.

4.3. *Inter-annual variation of the average NDVI in the mainland of China*

To visualize the features of the three NDVI datasets for the mainland of China, Figure 11 shows the inter-annual variation of NDVI averaged over mainland China. Compared to MODIS NDVI and GIMMS NDVI, GIMMS3g NDVI had the highest annual mean values intuitively, and GIMMS NDVI is smaller than the MODIS NDVI found in other research (Zhang et al. 2017; Gallo et al. 2005; Steven et al. 2003). The three datasets all show the same trend of NDVI in mainland China to prove the greening of vegetation. However, we can find that before 2000, the trend is stable and that there are no large fluctuations, as seen from the departure of the coefficient of determination (R^2) from 1.

The gentle, positive trends of GIMMS and GIMMS3g are similar before 2000. This indicates that there is no obvious variation in the overall vegetation of mainland China,

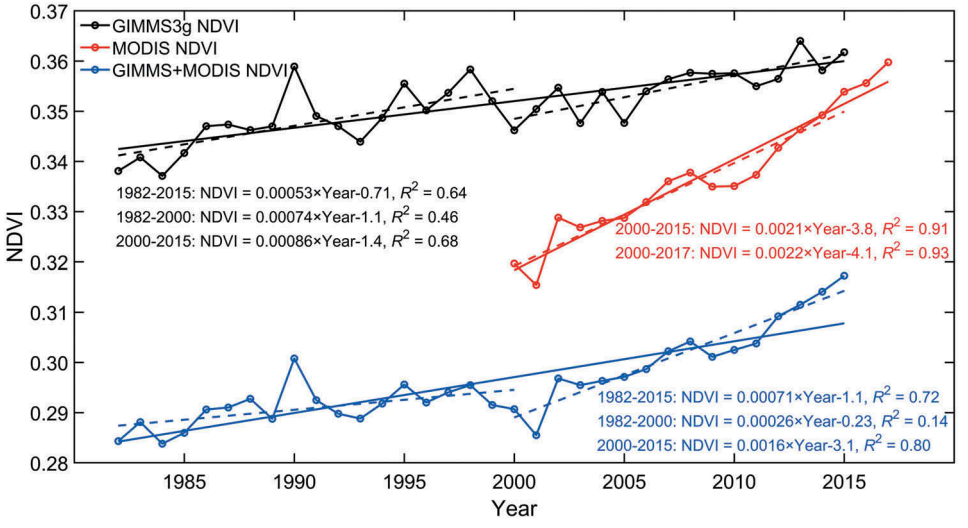

Figure 11. Inter-annual variations of the three NDVI datasets in mainland China. NDVI indicates that the range of vegetation is [0,1], and the ordinate on the ordinate here is set to [0.28,0.37], which only indicates the interval in which the average annual NDVI value of mainland China is located.

and even the growth rate level of GIMMS3g is a bit higher. Since 2000, NDVI datasets have shown a relatively obvious upward trend. For 2000 to 2015, GIMMS3g has performed more smoothly than MODIS. By comparing the data fitted by GIMMS and MODIS with GIMMS3g, the GIMMS+MODIS from 1982 to 2015 may overestimate the trend of NDVI growth. GIMMS3g and MODIS data show different changes in individual years, such as in 2008–2012. On the whole, the two long time-series datasets can better reflect the vegetation trends of mainland China. It is also found that the greening trend of vegetation coverage is distinct in the 2 years from 2015 to 2017, meaning that the vegetation development in mainland China is optimistic. The vegetation coverage in mainland China has been improved for the twenty-first century, and the sustainable development of vegetation cannot be ignored in the future.

On the scale of hydro-climatic partitions and ecosystems, the trends of the three NDVI datasets were compared; furthermore, the changes on vegetation cover in these basins are well explained (Figure 12). The NDVI values differ for different basins and data sources. A few basins have different and even striking opposite trends in some of the individual time intervals shown in Figure 12(a). For example, the trend of GIMMS3g is positive in the Lower Yangtze River, Southeastern River, and Pearl River, whereas the trends of GIMMS are negative, -0.19×10^{-3}, -0.39×10^{-3}, and -0.54×10^{-3} per year, and the differences in slope are 1.2×10^{-3}, 0.59×10^{-3}, and 1.2×10^{-3} per year during 1982–2000. The negative trend is slight and can be treated as having small fluctuations (tested by M-K method, $|Z| < 1.96$). The commonality shared by the three river basins is that they are all economically developed areas, and NDVI values are relatively large. Urbanization in these areas is more prominent, which is presumed to be related to NDVI vulnerability to population disturbances and the land cover changes. In the interval of 2000–2015, GIMMS3g and MODIS data also show opposite trends in three basins but differ from the previous three basins,

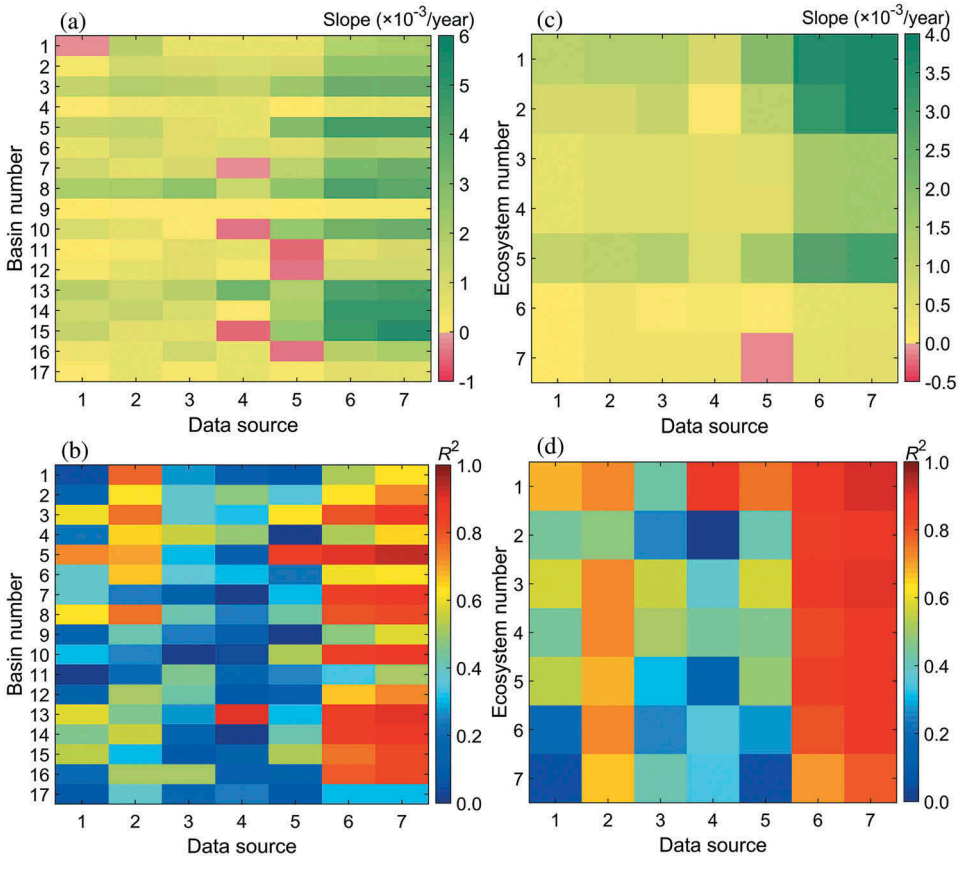

Figure 12. The Slope and R^2 of NDVI averaged in 17 basins and 7 ecosystems in 7 data sources. The names of the 17 basins correspond to the number codes referred to in Table 1. The numbers from 1 to 7 correspond to different ecosystems. 1: Farmland ecosystem; 2: Forest ecosystem; 3: Grassland ecosystem; 4: Water and wetland ecosystem; 5: Settlement ecosystem; 6: Desert ecosystem; and 7: Other ecosystems. In addition, the data sources represent the contrast of different time intervals for different NDVI datasets. 1: GIMMS3g 1982–2015; 2: GIMMS+MODIS 1982–2015; 3: GIMMS3g 1982–2000; 4: GIMMS 1982–2000; 5: GIMMS3g 2000–2015; 6: MODIS 2000–2015; 7: MODIS 2000–2017. (a) The Slope of NDVI averaged in 17 basins. (b) The R^2 of NDVI averaged in 17 basins. (c) The Slope of NDVI averaged in seven ecosystems. (d) The R^2 of NDVI averaged in seven ecosystems.

namely those of the Brahmaputra River, the Upper Yangtze River, and the Lancang River. Unlike before, the trends of GIMMS3g are negative, -0.55×10^{-3}, -0.39×10^{-3}, and -0.42×10^{-3} per year, whereas the trends of MODIS are positive, with corresponding differences of 0.81×10^{-3}, 1.1×10^{-3}, and 1.1×10^{-3} per year. The three basins are located in the southwestern part of China and are also areas with high NDVI values. In other studies, the vegetation in southwestern China should show a browning trend, indicating that MODIS data possibly overestimate the greening trends and underestimate the browning trends in this part of China, and GIMMS3g is more convincing (Pan et al. 2018). However, overall, the NDVI is not performing well in areas with high-vegetation coverage (Fensholt and Proud 2012). In the long-term sequence from 1982 to 2015, the overall trend is very similar, indicating that the fusion data are also possibly reliable. Only the mild trend

difference in the Songhua River is observed, showing that GIMMS3g is realized as a negative value, while the GIMMS+MODIS is a positive development. The Songhua River is a region that is affected strongly by human activities. Therefore, it is difficult to accurately judge the changes in the trend. The region has experienced a stage during which the vegetation is getting worse and better, and it is therefore hard to measure or conclude whether it is restored or improved. However, clearly it is certain that the region is already developing in the positive direction.

The R^2 for Middle and Lower Yangtze River except for those of GIMMS in 2000–1982 were close to 1, and the rest were lower. GIMMS3g has the highest R^2 in Lower Yellow River in 2000–2015, while MODIS only has a lower R^2 for the Brahmaputra River and basins of inland rivers in Inner Mongolia, while the rest are close to 1(Figure 12(b)).

Unlike the river basins, desert and other ecosystems in low-value areas have significant differences in trends (Figure 12(c)). In terms of ecosystems, the values of the GIMMS +MODIS NDVI from 1982 to 2015 are larger, and the differences are obvious in desert and other ecosystems. In 1982–2000, the most obvious difference between the two generations of GIMMS was the part of the farmland ecosystem; after 2000, GIMMS3g and MODIS had larger differences than for the farmland ecosystem. The MODIS data of desert ecosystems show an increasing trend, while GIMMS3g has a flat trend. In other ecosystems, the trend of GIMMS3g declines during the 2000–2015 period, although not obviously, while the MODIS data are reversed.

Figure 12(d) describes the R^2 of ecosystems at every stage. The values for GIMMS +MODIS from 1982 to 2015 are larger than for GIMMS3g, as obviously shown in desert and other ecosystems. In 1982–2000, the most significant difference between the two generations of GIMMS was the part of the farmland ecosystem; after 2000, GIMMS3g and MODIS had larger differences except for the farmland ecosystem.

From the perspective of R^2 (Figure 12(b,d)), the value of MODIS is generally higher, and GIMMS and GIMMS3g are almost at the same level. On the opposite trendiest parts, the R^2 is low, indicating that it is not sensitive to time, and the trend difference exists but is not so certain. In addition, compared with MODIS for 2000–2015 and 2000–2017, the R^2 has generally increased. The R^2 of GIMMS3g was generally lower than that of GIMMS+MODIS during 1982–2015.

4.4. NDVI trend analysis of ecosystems in the 17 basins

In the main, there is no noticeable browning in the ecosystem matching with universal cognition (Figure 1). In the long-term sequence from 1982 to 2015, the differences between GIMMS3g and the GIMMS+MODIS NDVI data are more markedly reflected in the farmland, forests, water and wetlands, and desert ecosystems in the Songhua River Basin, as well as desert and other ecosystems of Xinjiang's inland River Basin (Table 3). In addition, the opposite trend is present in the forest ecosystem of the Brahmaputra and other ecosystems of the Lancang River Basin. Before 2000, all ecosystems in the lower Yangtze River Basin and the Pearl River Basin exhibited opposite trends in GIMMS and GIMMS3g. The forest ecosystem in the Lancang River Basin faced the same situation, that is, the GIMMS+MODIS is expressed as negative, while the GIMMS3g is greening. The opposite was found in forest and grassland ecosystems of the southeast Rivers Basin. It is recognized that the two datasets together indicated browning in the farmland, water and

Table 3. The *Z*-value of the ecosystems in 17 basins in mainland China.

Basin		1	2	3	4	5	6	7	8	9	10	11	12	13	14	15	16	17
GIMMS+MODIS 1982-2015	FL	1.48	3.56	4.31	3.71	4.15	3.05	1.74	3.96		1.89		1.93	3.43	3.83	2.62	2.13	2.71
	FR	1.48	2.42	4.50	1.44	3.75	3.07	2.51	3.99		2.38	0.70	1.59	2.90	3.00	2.12	1.89	1.88
	GL	1.57	2.96	4.36	1.48	3.60	3.19	2.54	3.80	1.22	2.31	1.60	1.80	3.84	3.05	2.46	1.36	1.71
	WW	1.17	3.52	3.26	1.53	3.87	2.66	0.79	3.26	1.02	1.51	1.74	1.37	2.55	3.09	1.34	1.51	1.83
	DS	1.75	3.07	3.52		3.65		0.27	3.62		0.46			2.87	2.07	1.54		
	SM	3.28	3.24		0.57	4.14	2.55			1.10		1.09	2.45					0.38
	OE				0.53	1.99	2.99			1.36		1.49	2.06				1.81	0.11
GIMMS3g 1982-2015	FL	-0.88	1.28	3.03	3.26	3.46	2.94	2.27	3.57		1.96		1.39	3.57	3.14	3.29	1.97	1.60
	FR	-0.33	1.10	3.27	1.04	3.24	1.52	2.80	3.11		2.33	-0.21	0.99	3.39	2.20	2.80	1.49	0.86
	GL	0.19	0.92	3.20	0.87	3.50	1.72	2.59	3.13	1.02	2.84	0.75	0.70	3.98	1.90	2.68	0.52	0.76
	WW	-0.59	1.33	2.03	0.58	3.06	1.35	1.33	2.76	0.51	1.85	0.37	1.35	2.42	2.39	2.64	0.32	1.02
	DS	-0.58	0.92	2.55		2.42		1.01	3.23		1.11			2.83	1.44	1.93		
	SM	1.48	1.63		-0.26	3.76	1.65			0.60		0.34	1.73					0.92
	OE				-0.22	2.84	1.75			1.02		0.52	1.04				-0.02	0.88
GIMMS 1982-2000	FL	0.64	1.49	1.58	2.03	0.79	1.04	-0.02	1.11		-0.33		0.38	0.48	0.33	-0.28	0.35	1.59
	FR	0.37	1.10	1.45	1.24	0.38	1.10	-0.43	0.76		-0.40	0.01	0.40	0.05	0.06	-0.51	0.34	0.66
	GL	0.77	1.30	1.45	1.09	0.73	1.13	-0.34	1.03	0.70	-0.48	1.30	0.41	0.24	0.18	-0.26	0.58	1.01
	WW	0.72	1.44	1.07	1.23	1.09	0.99	0.00	0.93	0.70	-0.10	1.15	0.32	0.37	0.43	-0.70	0.53	1.05
	DS	0.84	1.23	1.22		1.01		-0.25	0.97		-0.32			0.48	-0.10	-0.66		
	SM	1.10	1.20		0.39	1.49	0.80			0.39		0.41	0.79					0.37
	OE				0.45	0.76	0.88			0.47		0.87	0.55				0.95	0.15
GIMMS3g 1982-2000	FL	0.61	1.87	2.15	2.79	1.39	1.51	1.20	2.31		-0.04		1.25	1.79	1.14	1.14	1.51	1.97
	FR	1.19	1.73	2.03	1.81	1.03	1.47	1.04	1.45		0.24	1.02	1.58	1.61	0.91	0.74	1.63	1.04
	GL	0.75	1.47	1.81	1.39	1.17	1.39	1.09	1.51	1.16	0.44	1.68	1.06	1.73	1.05	0.57	1.28	0.86
	WW	0.69	1.52	1.36	1.07	1.76	1.39	0.75	1.52	0.69	-0.22	1.02	0.91	1.08	0.83	0.83	1.08	1.01
	DS	0.75	1.61	1.77		1.52		0.28	2.18		-0.60			1.43	0.21	0.13		
	SM	0.81	1.22		0.31	1.81	1.10			0.45		0.89	1.25					0.41
	OE				0.48	0.89	0.81			0.65		1.14	1.18				1.13	0.31
GIMMS3g 2000-2015	FL	0.35	1.07	1.58	1.82	2.31	2.25	1.03	1.59		-0.04		-0.00	1.37	2.17	2.17	0.42	0.57
	FR	0.15	0.92	2.40	-0.37	2.37	0.55	1.84	1.91		2.22	-0.77	-0.43	1.42	1.40	1.89	-0.00	0.57
	GL	1.08	1.28	2.29	-0.04	2.57	0.71	1.73	1.87	0.01	2.52	-0.32	-0.19	1.91	1.04	1.80	-0.68	0.53
	WW	0.26	1.47	1.33	-0.02	1.80	0.38	0.49	1.41	0.02	2.05	-0.21	0.43	0.79	1.68	2.06	-0.44	0.83
	DS	0.40	0.75	1.25		1.31		0.41	1.27		1.21			0.83	1.29	1.84		
	SM	2.06	1.84		-0.24	2.52	0.66			0.36		0.09	0.49					0.56
	OE				-0.21	2.07	1.16			0.59		-0.24	-0.13				-1.00	0.57
MODIS 2000-2015	FL	1.53	2.34	2.39	2.24	3.16	2.50	2.07	2.45		2.36		1.53	2.88	3.25	2.72	2.06	1.23
	FR	1.52	2.00	3.23	0.37	3.49	1.95	3.24	3.03		3.08	1.06	1.21	3.13	2.88	2.61	1.61	1.43
	GL	1.50	2.07	2.99	0.63	3.14	1.64	3.17	2.51	0.77	2.95	0.28	1.21	3.69	2.72	2.71	0.67	1.12
	WW	1.03	2.28	2.12	0.51	2.83	1.22	1.29	2.04	0.54	1.75	0.60	1.45	2.10	2.57	2.21	0.98	1.44
	DS	1.62	2.06	1.89		2.36		0.92	2.18		1.02			2.31	2.05	2.19		
	SM	2.56	2.35		0.31	3.12	1.63			0.74		0.39	1.67					0.91
	OE				0.50	2.04	1.66			1.09		0.76	1.41				0.48	0.78
MODIS 2000-2017	FL	1.87	2.76	2.87	2.78	3.51	2.89	2.39	2.63		2.90		2.10	3.21	3.71	3.33	2.72	1.62
	FR	2.13	2.50	3.74	0.76	3.94	2.29	3.82	3.58		3.65	1.51	1.57	3.69	3.39	3.27	2.20	1.89
	GL	1.48	2.49	3.48	1.12	3.50	1.73	3.67	3.08	1.24	3.51	0.76	1.39	4.11	3.15	3.36	1.13	1.04
	WW	1.28	2.69	2.52	0.83	3.29	1.25	1.50	2.14	0.81	2.29	0.90	1.61	2.28	3.05	2.79	1.36	1.52
	DS	1.93	2.41	2.39		2.80		1.32	2.29		1.51			2.60	2.45	2.74		
	SM	2.69	2.79		0.52	3.62	1.62			0.85		0.56	1.72					1.04
	OE				0.78	2.43	1.60			1.26		1.15	1.47				0.82	0.94
$Z \leq 0$						$0<Z<1.96$							$1.96 \leq Z$					

A blank indicates that the proportion of the ecosystem in this area is so tiny that it can be ignored. The names of the basins correspond to the number codes referred to in Table 1. Green represents $Z \geq 1.96$, yellow represents $Z > 0$ and $Z < 1.96$, and light blue represents $Z \leq 0$. FL: the farmland ecosystem; FR: the forest ecosystem; GL: the grassland ecosystem; WW: the water and wetland ecosystem; SM: the settlement ecosystem; DE: the desert ecosystem; OE: the other ecosystems.

wetland, and desert ecosystems of Southeastern River Basin, illustrating the negative trend of vegetation in Southeastern River Basin before 2000 and also revealing the major ecosystems that lead to the NDVI decline. The gap between MODIS data and GIMMS3g data in Xinjiang after 2000 is mainly due to the negative trend of GIMMS3g in all ecosystems except farmland. The basins of the inland rivers in northern Tibet, however, mainly comprise grassland and water and wetland ecosystems. Farmland ecosystems show differences with those of Southeastern Rivers Basin. The Lancang River Basin, the Brahmaputra River Basin, and the Upper Yangtze River Basin have the same vegetation development in the settlement ecosystem, and the rest of the ecosystems have minor differences. Comparing the 2000–2015 and 2000–2017 changes of MODIS NDVI data, it is found that the greening is significant and that the farmland and forest ecosystems are generally outstanding.

The main reasons for the different NDVI trends in different basins and ecosystems are that the driving impact factors of the vegetation in different regions and different vegetation types are different. For instance, the main driving force for vegetation change in North China is the precipitation while for South China, temperature plays the main role (Piao et al. 2015; Tian et al. 2015b; Bin et al. 2015). In densely populated areas, the impact of climate change is less evident. The impact of human activities on vegetation variation cannot be ignored in fast urbanized areas (Gong et al. 2010). The implementation of ecological engineering in recent decades should be an important driving force for vegetation restoration in some areas (Liu et al. 2015; Chen et al. 2019).

5. Discussion

The worldwide NDVI datasets currently available are mainly AVHRR NDVI, MODIS NDVI, and SPOT-VGT NDVI, as well as NDVI data extracted from Landsat data. They have their own characteristics because of different sensors and different resolutions. In this paper, we chose the more popular NDVI sets, including the integration of GIMMS and MODIS data and the research period was established from 1982 to 2015/2017. Adding more NDVI datasets may better reflect the uncertainty of vegetation change analysis brought about by the data. The change of vegetation is different between months and seasons. The sensitivity of different NDVI data sets in different seasons is also different, which is a part of the research remained to be done. In addition, different NDVI datasets have different responses to climate change. In this study, different NDVI datasets were used to describe the spatial distribution of vegetation activities and the different trends of vegetation change, but their correlation with climate change was not explored.

Different vegetation types respond differently to climate change and human activities so that the NDVI trends of different ecosystems are different. The same ecosystem's NDVI trends also have significant differences in different regions. For instance, according to 1982–2015 GIMMS3g NDVI, forest ecosystems showed a downward trend in Songhua River and Brahmaputra, but it showed a significant upward trend in Lower Yellow River and Pearl River. Different NDVI datasets have different performances in the same period and ecosystem. For example, for the farmland ecosystem in Lower Yellow River from 2000 to 2015, GIMMS3g showed a slight degradation trend, while MODIS NDVI showed a significant increase.

With the large-scale urbanization process in the late 1990s in China, cities and buildings increased, and the cultivated land decreased (Tian, Zhuang, and Liu 2003; Deng et al. 2015; Jiyuan et al., 2012). NDVI shows that the sudden change in vegetation decreased in the cities of China (Sun 2012). In addition, since the implementation of the project of returning farmland to forests and grasslands in 1999, the afforestation area in China has continued to rise, which has greatly promoted the increase of vegetation cover in China (Liu et al. 2015; Xin, Xu, and Zheng 2008). Studies have shown that China's afforestation policy and intensive agriculture have made tremendous contributions to greening in the world (Chen et al. 2019).

Figure 13(a) shows the increase of NDVI over the past three decades and the temperature of mainland China has been rising which is the same as NDVI (Figure 13(b)). Vegetation cover increased as the temperature gradually increased (Kawabata, Ichii, and Yamaguchi 2001; Eastman et al. 2013) while there is no obvious change trend in annual precipitation (Figure 13(c)). The proportion of rural population in China shows a sustained downward trend from 1982 to 2015. In 2011, the proportion of rural population in China was less than 50% for the first time, reaching 48.7%, which was the first time in history that urban population exceeded rural population (Figure 13(d)). As the proportion of rural population decreases, the social and economic pressure on the growth of local vegetation

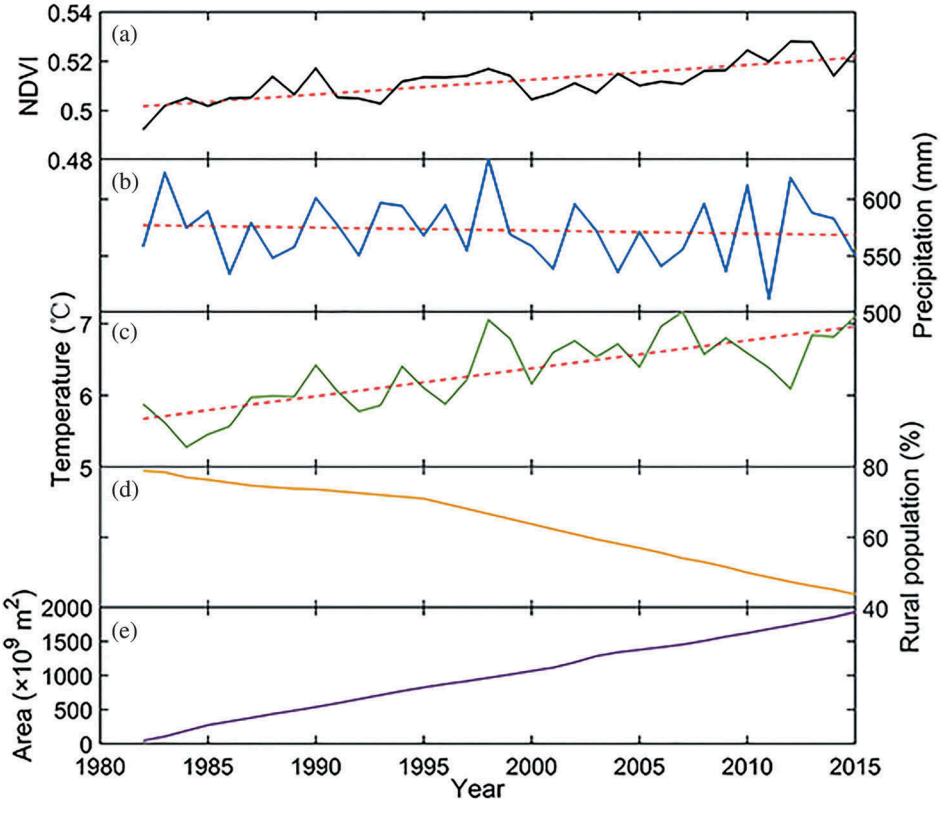

Figure 13. The 1982–2015 inter-annual variation of (a) NDVI; (b) Annual precipitation; (c) Annual temperature; (d) The proportion of rural population; (e) Cumulative afforestation area.

has been alleviated to a certain extent, which can improve the local vegetation coverage. The increase of NDVI in China is also closely related to China's afforestation projects (Wenhua 2004; Gao et al. 2014). In recent years, China's cumulative afforestation area has shown a significant upward trend (Figure 13(e)), which is also one of the main reasons for the increase in vegetation.

Human activities gradually intensify, which has an impact on natural resources and ecological environment. Greenhouse gases in the atmosphere have increased significantly, leading to global warming. Vegetation growth is mainly affected by water and heat (Richardson et al. 2013). In recent years, the increase of extreme weather in China will also have a response effect on vegetation in China. Human activities were frequent in China around 2000. There are great regional differences in vegetation change in China, and the time of human activities in different regions is also different (Piao et al. 2015). We selected one segmentation point in 2000 nationwide and may have overlooked regional differences. The method of mutation point test can be further used. The mutation points of vegetation change in different areas were detected to better analyse the trend change of NDVI. This paper only analyses the change of vegetation coverage in China and does not study the correlation between other meteorological factors or human activities. In the future, with the increasing impact of climate change and human beings on the Earth, how vegetation will respond to these related factors remains to be studied.

6. Conclusions

In this study, MODIS NDVI and GIMMS NDVI are fused using linear regression equations to form 1982–2015 composite NDVI data that are treated as a group with GIMMS3g NDVI, which is also the case for 1982–2000 GIMMS NDVI and GIMMS3g NDVI, 2000–2015 GIMMS3g NDVI and MODIS NDVI, to which are attached 2000–2017 MODIS NDVI data. Linear least squares regression trend analysis and M-K trend analysis of annual average NDVI were used in these groups. To test the performance of the long-term dataset from 1982 to the present in mainland China, it is assumed that the quality of the updated MODIS products is higher. The results show that the trend patterns of the three datasets are different, reflecting the performances of individual regions.

With 2000 as the dividing point, the trend of vegetation in mainland China has staged characteristics. GIMMS and GIMMS3g show a more consistent range of regression slopes before 2000; GIMMS3g and MODIS have generally inconsistent slope values after 2000, while the greening trend exhibited by MODIS is higher than the positive slope of GIMMS3g. In the humid and sub-humid areas, which are high-density vegetation areas in mainland China, the trend of significant differences in regression slope values is more obvious. In the region of the northeast and southwest basins with high NDVI values, differences are observed. The low-vegetation coverage of the inner river regions in the northwest also shows differences, although it is not as obvious as the high-value area. This indicates that NDVI datasets show greater uncertainty in regions with high- or low-vegetation coverage. We believe that the combination of GIMMS NDVI and MODIS NDVI has certain advantages.

In general, vegetation activities on the mainland of China have been active and positive for nearly 40-recent years, only differing in the increasing rates in various basins and ecosystems and in individual areas in decline. The most obvious greening area is Yellow River and the middle reaches of Yangtze River, while the areas experiencing

significant declines are in the Yangtze River Delta and the Pearl River Delta. In terms of ecosystems, the areas where vegetation activities are significantly enhanced are farmland and forest ecosystems that are mainly distributed in the eastern monsoon basin. The areas experiencing declines are the desert and grassland ecosystems of the northwest region, besides the northeast and southeast forest ecosystems. We can hardly find a tendency to decline at low resolutions or for averages over larger regions. Therefore, research with different resolutions and at different scales is necessary.

Disclosure statement

No potential conflict of interest was reported by the authors.

Funding

This study was supported by the National Natural Science Foundation of China [No. 51879009], the Second Tibetan Plateau Scientific Expedition and Research Program [No.2019QZKK0405], the National Key Research and Development Program of China [No. 2018YFE0196000].

References

Adami, M., S. Bernardes, E. Arai, R. M. Freitas, Y. E. Shimabukuro, F. D. Espírito-Santo and L. O. Anderson. 2018. "Seasonality of Vegetation Types of South America Depicted by Moderate Resolution Imaging Spectroradiometer (MODIS) Time Series." *International Journal of Applied Earth Observation and Geoinformation* 69: 148–163. doi:10.1016/j.jag.2018.02.010.

Balato, N., C. Patruno, F. P. D'Errico, and A. Balato. 2008. "Global Warming and Its Effect on Dermatology and Plants." *Archives of Dermatology* 144: 1016. doi:10.1001/archderm.144.8.1016.

Beck, H. E., T. R. McVicar, A. I. J. M. van Dijk, J. Schellekens, R. A. M. de Jeu, and L. A. Bruijnzeel. 2011. "Global Evaluation of Four AVHRR–NDVI Data Sets: Intercomparison and Assessment against Landsat Imagery." *Remote Sensing of Environment* 115: 2547–2563. doi:10.1016/j.rse.2011.05.012.

Bin, H., C. Aifang, W. Honglin, and W. Qianfeng. 2015. "Dynamic Response of Satellite-derived Vegetation Growth to Climate Change in the Three North Shelter Forest Region, in China." *Remote Sensing* 7 (8): 9998–10016. doi:10.3390/rs70809998.

Bonan, G. B. 2008. "Forests and Climate Change: Forcings, Feedbacks, and the Climate Benefits of Forests." *Science* 320: 1444–1449. doi:10.1126/science.1155121.

Butt, B., M. D. Turner, A. Singh, and L. Brottem. 2011. "Use of MODIS NDVI to Evaluate Changing Latitudinal Gradients of Rangeland Phenology in Sudano-Sahelian West Africa." *Remote Sensing of Environment* 115: 3367–3376. doi:10.1016/j.rse.2011.08.001.

Chen, C., T. Park, X. Wang, S. Piao, B. Xu, R. K. Chaturvedi, … H. Tømmervik. 2019. "China and India Lead in Greening of the World through Land-use Management." *Nature Sustainability* 2 (2): 122. doi:10.1038/s41893-019-0220-7.

Dai, L., Y. Wang, D. Su, L. Zhou, D. Yu, B. J. Lewis, and L. Qi. 2011. "Major Forest Types and the Evolution of Sustainable Forestry in China." *Environmental Management* 48 (6): 1066–1078. doi:10.1007/s00267-011-9706-4.

Dai, S., B. Zhang, and H. Wang. 2010. "Spatio-temporal Change of Vegetation Index NDVI in Northwest China and Its Influencing Factors." *Journal of Geo-Information Science* 3: 003. doi:10.3724/sp.j.1047.2010.00315.

Dardel, C., L. Kergoat, P. Hiernaux, E. Mougin, M. Grippa, and C. J. Tucker. 2014. "Re-greening Sahel: 30years of Remote Sensing Data and Field Observations (Mali, Niger)." *Remote Sensing of Environment* 140: 350–364. doi:10.1016/j.rse.2013.09.011.

de Beurs, K. M., and G. M. Henebry. 2004. "Trend Analysis of the Pathfinder AVHRR Land (PAL) NDVI Data for the Deserts of Central Asia." *IEEE Geoscience and Remote Sensing Letters* 1 (4): 282–286. doi:10.1109/LGRS.2004.834805.

De Jong, R., S. de Bruin, A. de Wit, M. E. Schaepman, and D. L. Dent. 2011. "Analysis of Monotonic Greening and Browning Trends from Global NDVI Time-series." *Remote Sensing of Environment* 115: 692–702. doi:10.1016/j.rse.2010.10.011.

Deng, X., J. Huang, S. Rozelle, J. Zhang, and Z. Li. 2015. "Impact of Urbanization on Cultivated Land Changes in China." *Land Use Policy* 45 (45): 1–7. doi:10.1016/j.landusepol.2015.01.007.

Du, J., J. Shu, Y. Wang, Y. Li, L. Zhang, and Y. Guo. 2014. "Comparison of GIMMS and MODIS Normalized Vegetation Index Composite Data for Qing-Hai-Tibet Plateau." *The Journal of Applied Ecology* 25: 533–544. doi:10.13287/j.1001-9332.2014.0056.

Eastman, J., F. Sangermano, E. Machado, J. Rogan, and A. Anyamba. 2013. "Global Trends in Seasonality of Normalized Difference Vegetation Index (NDVI), 1982–2011." *Remote Sensing* 5 (10): 4799–4818. doi:10.3390/rs5104799.

Fang, J. 2004. "Increasing Terrestrial Vegetation Activity in China, 1982–1999." *Science in China Series C* 47: 229. doi:10.1007/BF03182768.

Fensholt, R., K. Rasmussen, T. T. Nielsen, and C. Mbow. 2009. "Evaluation of Earth Observation Based Long Term Vegetation Trends — Intercomparing NDVI Time Series Trend Analysis Consistency of Sahel from AVHRR GIMMS, Terra MODIS and SPOT VGT Data." *Remote Sensing of Environment* 113: 1886–1898. doi:10.1016/j.rse.2009.04.004.

Fensholt, R., and S. R. Proud. 2012. "Evaluation of Earth Observation Based Global Long Term Vegetation Trends — Comparing GIMMS and MODIS Global NDVI Time Series." *Remote Sensing of Environment* 119: 131–147. doi:10.1016/j.rse.2011.12.015.

Fensholt, R., T. Langanke, K. Rasmussen, A. Reenberg, S. D. Prince, C. Tucker, R. J. Scholes, et al. 2012. "Greenness in Semi-arid Areas across the Globe 1981–2007 — An Earth Observing Satellite Based Analysis of Trends and Drivers." *Remote Sensing of Environment* 121: 144–158. doi:10.1016/j.rse.2012.01.017.

Ferrara, R. M., C. Fiorentino, N. Martinelli, P. Garofalo, and G. Rana. 2010. "Comparison of Different Ground-based NDVI Measurement Methodologies to Evaluate Crop Biophysical Properties." *Italian Journal of Agronomy* 5: 145–154. doi:10.4081/ija.2010.145.

Gajewski, K. 2015. "Impact of Holocene Climate Variability on Arctic Vegetation." *Global and Planetary Change* 133: 272–287. doi:10.1016/j.gloplacha.2015.09.006.

Gallo, K., L. Ji, B. Reed, J. Dwyer, and J. Eidenshink. 2004. "Comparison of MODIS and AVHRR 16-day Normalized Difference Vegetation Index Composite Data." *Geophysical Research Letters* 31: L07502. doi:10.1029/2003GL019385.

Gallo, K., L. Ji, B. Reed, J. Eidenshink, and J. Dwyer. 2005. "Multi-platform Comparisons of MODIS and AVHRR Normalized Difference Vegetation Index Data." *Remote Sensing of Environment* 99: 221–231. doi:10.1016/j.rse.2005.08.014.

Gao, Y., X. Zhu, G. Yu, N. He, Q. Wang, and J. Tian. 2014. "Water Use Efficiency Threshold for Terrestrial Ecosystem Carbon Sequestration in China under Afforestation." *Agricultural and Forest Meteorology* 195: 32–37. doi:10.1016/j.agrformet.2014.04.010.

Gitelson, A. A. 2004. Wide dynamic range vegetation index for remote quantification of biophysical characteristics of vegetation. Journal of Plant Physiology,161(2), 0–173. doi: 10.1029/2003gl019034

Gong, H. S., M. S. Chung, J. H. Oh, Y. H. Lee, S. H. Kim, and G. H. Baek. 2010. "An Analysis on Eco-environmental Effect of Vegetation in Urbanized Areas." *Ecology & Environmental Sciences* 19 (11): 2737–2742. doi:10.1016/S1872-5813(11)60001-7.

Guenther, A. 2002. "The Contribution of Reactive Carbon Emissions from Vegetation to the Carbon Balance of Terrestrial Ecosystems." *Chemosphere* 49: 837–844. doi:10.1016/S0045-6535(02)00384-3.

Heumann, B. W., J. W. Seaquist, L. Eklundh, and P. Jönsson. 2007. "AVHRR Derived Phenological Change in the Sahel and Soudan, Africa, 1982–2005." *Remote Sensing of Environment* 108: 385–392. doi:10.1016/j.rse.2006.11.025.

Hill, M. J., P. J. Vickery, E. P. Furnival, and G. E. Donald. 1999. "Pasture Land Cover in Eastern Australia from NOAA-AVHRR NDVI and Classified Landsat TM." *Remote Sensing of Environment* 67: 32–50. doi:10.1016/S0034-4257(98)00075-3.

Holben, B. N. 2007. "Characteristics of Maximum-value Composite Images from Temporal AVHRR Data." *International Journal of Remote Sensing* 7: 1417–1434. doi:10.1080/01431168608948945.

Huete, A., K. Didan, T. Miura, E. P. Rodriguez, X. Gao, and L. G. Ferreira. 2002. "Overview of the Radiometric and Biophysical Performance of the MODIS Vegetation Indices." *Remote Sensing of Environment* 83: 195–213. doi:10.1016/S0034-4257(02)00096-2.

Huete, A. R., H. Q. Liu, K. Batchily, and W. V. Leeuwen. 1997. "A Comparison of Vegetation Indices over a Global Set of TM Images for EOS-MODIS." *Remote Sensing of Environment* 59: 440–451. doi:10.1016/S0034-4257(96)00112-5.

Jamali, S., P. Jönsson, L. Eklundh, J. Ardö, and J. Seaquist. 2015. "Detecting Changes in Vegetation Trends Using Time Series Segmentation." *Remote Sensing of Environment* 156: 182–195. doi:10.1016/j.rse.2014.09.010.

Jarlan, L., S. Mangiarotti, E. Mougin, P. Mazzega, P. Hiernaux, and V. Ledantec. 2008. "Assimilation of SPOT/VEGETATION NDVI Data into a Sahelian Vegetation Dynamics Model." *Remote Sensing of Environment* 112: 1381–1394. doi:10.1016/j.rse.2007.02.041.

Jiang, W., L. Yuan, W. Wang, R. Cao, Y. Zhang, and W. Shen. 2015. "Spatio-temporal Analysis of Vegetation Variation in the Yellow River Basin." *Ecological Indicators* 51: 117–126. doi:10.1016/j.ecolind.2014.07.031.

Jiyuan, Z, and Y. Qian. 2012. "Regional Differences of China's Urban Expansion from Late 20th to Early 21st Century Based on Remote Sensing Information." *Chinese Geographical Science* 22 (1): 1–14. doi:10.1007/s11769-012-0510-8.

John, W., and H. David, 2000. "Measuring Vegetation (NDVI & EVI)." Accessed 2 February 2019. https://earthobservatory.nasa.gov/features/MeasuringVegetation

Ju, J., and J. G. Masek. 2016. "The Vegetation Greenness Trend in Canada and US Alaska from 1984–2012 Landsat Data." *Remote Sensing of Environment* 176: 1–16. doi:10.1016/j.rse.2016.01.001.

Kaufman, Y. J., and D. Tanré. 1996. "Strategy for Direct and Indirect Methods for Correcting the Aerosol Effect on Remote Sensing: From AVHRR to EOS-MODIS." *Remote Sensing of Environment* 55: 65–79. doi:10.1016/0034-4257(95)00193-X.

Kawabata, A., K. Ichii, and Y. Yamaguchi. 2001. "Global Monitoring of Interannual Changes in Vegetation Activities Using Ndvi and Its Relationships to Temperature and Precipitation." *International Journal of Remote Sensing* 22 (7): 1377–1382. doi:10.1080/01431160119381.

Kendall, M. G. 1975. *Rank Correlation Methods*. London: Griffin.

Lang, Y., A. Ye, W. Gong, C. Miao, Z. Di, J. Xu, Y. Liu, L. Luo, and Q. Duan. 2014. "Evaluating Skill of Seasonal Precipitation and Temperature Predictions of NCEP CFSv2 Forecasts over 17 Hydroclimatic Regions in China." *Journal of Hydrometeorology* 15 (4): 1546–1559. doi:10.1175/JHM-D-13-0208.1.

Le Maire, G., C. François, K. Soudani, H. Davi, V. Le Dantec, B. Saugier, and E. Dufrêne. 2006. "Forest Leaf Area Index Determination: A Multiyear Satellite-independent Method Based on Within-stand Normalized Difference Vegetation Index Spatial Variability." *Journal of Geophysical Research: Biogeosciences* 111: G2. doi:10.1029/2005jg000122.

Lenzen, M., -Y.-Y. Sun, F. Faturay, Y.-P. Ting, A. Geschke, and A. Malik. 2018. "The Carbon Footprint of Global Tourism." *Nature Climate Change* 8: 522–528. doi:10.1038/s41558-018-0141-x.

Li, D., M. Pan, Z. Cong, L. Zhang, and E. Wood. 2013. "Vegetation Control on Water and Energy Balance within the Budyko Framework." *Water Resources Research* 49 (2): 969–976. doi:10.1002/wrcr.20107.

Li, D., S. Wu, L. Liu, Y. Zhang, and S. Li. 2018. "Vulnerability of the Global Terrestrial Ecosystems to Climate Change." *Glob Change Biol* 24: 4095–4106. doi:10.1111/gcb.14327.

Li, F., Y. Zeng, X. Li, Q. Zhao, and B. Wu. 2014. "Remote Sensing Based Monitoring of Interannual Variations in Vegetation Activity in China from 1982 to 2009." *Science China Earth Sciences* 57: 1800–1806. doi:10.1007/s11430-014-4883-7.

Lin, Q. H., L. R. Sun, X. Z. Wang, and L. L. Hu. 2013. "Spatio-Temporal Variation of Vegetation NDVI in China from 2001 to 2011." *Advanced Materials Research* 4: 610–613. doi:10.4028/www.scientific.net/AMR.610-613.3752.

Liu, S., T. Wang, J. Guo, J. Qu, and P. An. 2010. "Vegetation Change Based on SPOT-VGT Data from 1998 to 2007, Northern China." *Environmental Earth Sciences* 60: 1459–1466. doi:10.1007/s12665-009-0281-4.

Liu, Y., X. Liu, H. Yi'na, S. Li, J. Peng, and Y. Wang. 2015. "Analyzing Nonlinear Variations in Terrestrial Vegetation in China during 1982–2012." *Environmental Monitoring and Assessment* 187 (11): 722. doi:10.1007/s10661-015-4922-7.

Liu, Z., C. Wu, Y. Liu, X. Wang, B. Fang, W. Yuan, and Q. Ge. 2017. "Spring Green-up Date Derived from GIMMS3g and SPOT-VGT NDVI of Winter Wheat Cropland in the North China Plain." *ISPRS Journal of Photogrammetry and Remote Sensing* 130: 81–91. doi:10.1016/j.isprsjprs.2017.05.015.

Lunetta, R. S., J. F. Knight, J. Ediriwickrema, J. G. Lyon, and L. D. Worthy. 2006. "Land-cover Change Detection Using Multi-temporal MODIS NDVI Data." *Remote Sensing of Environment* 105: 142–154. doi:10.1016/j.rse.2006.06.018.

Mann, H. B. 1945. "Nonparametric Tests against Trend." *Econometrica: Journal of the Econometric Society* 13: 245–259. doi:10.2307/1907187.

Mao, D., Z. Wang, L. Luo, and C. Ren. 2012a. "Integrating AVHRR and MODIS Data to Monitor NDVI Changes and Their Relationships with Climatic Parameters in Northeast China." *International Journal of Applied Earth Observation and Geoinformation* 18: 528–536. doi:10.1016/j.jag.2011.10.007.

Mao, Y., A. Ye, and J. Xu. 2012b. "Using Land Use Data to Estimate the Population Distribution of China in 2000." *GIScience & Remote Sensing* 49 (6): 822–853. doi:10.2747/1548-1603.49.6.822.

Miura, T. 2002. "Overview of the Radiometric and Biophysical Performance of the MODIS Vegetation Indices." *Remote Sensing of Environment* 83: 195–213. doi:10.1016/S0034-4257(02)00096-2.

Montandon, L., and E. Small. 2008. "The Impact of Soil Reflectance on the Quantification of the Green Vegetation Fraction from NDVI." *Remote Sensing of Environment* 112: 1835–1845. doi:10.1016/j.rse.2007.09.007.

Montgomery, D. C., E. A. Peck, and G. G. Vining. 2012. *Introduction to Linear Regression Analysis*. Vol. 821. John Wiley & Sons.

Myneni, R. B., F. G. Hall, P. J. Sellers, and A. L. Marshak. 1995. "The Interpretation of Spectral Vegetation Indexes." *IEEE Transactions on Geoscience and Remote Sensing* 33: 481–486. doi:10.1109/36.377948.

Neeti, N., and J. R. Eastman. 2011. "A Contextual Mann-Kendall Approach for the Assessment of Trend Significance in Image Time Series." *Transactions in GIS* 15 (5): 599–611. doi:10.1111/j.1467-9671.2011.01280.x.

Pan, N., X. Feng, B. Fu, S. Wang, F. Ji, and S. Pan. 2018. "Increasing Global Vegetation Browning Hidden in Overall Vegetation Greening: Insights from Time-varying Trends." *Remote Sensing of Environment* 214: 59–72. doi:10.1016/j.rse.2018.05.018.

Peel, M. C., B. L. Finlayson, and T. A. McMahon. 2007. "Updated World Map of the Köppen-Geiger Climate Classification." *Hydrology and Earth System Sciences* 11: 1633–1644. doi:10.5194/hess-11-1633-2007.

Peng, S., A. Chen, L. Xu, C. Cao, J. Fang, R. B. Myneni, J. E. Pinzon, C. J. Tucker, and S. Piao. 2011. "Recent Change of Vegetation Growth Trend in China." *Environmental Research Letters* 6: 044027. doi:10.1088/1748-9326/6/4/044027.

Pettorelli, N., J. O. Vik, A. Mysterud, J. M. Gaillard, C. J. Tucker, and N. C. Stenseth. 2005. "Using the Satellite-derived NDVI to Assess Ecological Responses to Environmental Change." *Trends in Ecology & Evolution* 20: 503–510. doi:10.1016/j.tree.2005.05.011.

Piao, S. 2003. "Interannual Variations of Monthly and Seasonal Normalized Difference Vegetation Index (NDVI) in China from 1982 to 1999." *Journal of Geophysical Research* 108. doi:10.1029/2002JD002848.

Piao, S., G. Yin, J. Tan, L. Cheng, M. Huang, Y. Li, R. Liu, et al. 2015. "Detection and Attribution of Vegetation Greening Trend in China over the Last 30 Years." *Global Change Biology* 21: 1601–1609. doi:10.1111/gcb.12795.

Pinzon, J., and C. Tucker. 2014. "A Non-Stationary 1981–2012 AVHRR NDVI3g Time Series." *Remote Sensing* 6: 6929–6960. doi:10.3390/rs6086929.

Pouliot, D., R. Latifovic, and I. Olthof. 2009. "Trends in Vegetation NDVI from 1 Km AVHRR Data over Canada for the Period 1985–2006." *International Journal of Remote Sensing* 30 (1): 149–168. doi:10.1080/01431160802302090.

Richardson, A. D., T. F. Keenan, M. Migliavacca, Y. Ryu, O. Sonnentag, and M. Toomey. 2013. "Climate Change, Phenology, and Phenological Control of Vegetation Feedbacks to the Climate System." *Agricultural and Forest Meteorology* 169: 156–173. doi:10.1016/j.agrformet.2012.09.012.

Sarkar, S., and M. Kafatos. 2004. "Interannual Variability of Vegetation over the Indian Sub-continent and Its Relation to the Different Meteorological Parameters." *Remote Sensing of Environment* 90: 268–280. doi:10.1016/j.rse.2004.01.003.

Solano, R., K. Didan, A. Jacobson, and A. Huete. 2010. "MODIS Vegetation Index User's Guide (MOD13 Series)." *Vegetation Index and Phenology Lab, the University of Arizona* 1–38. doi:10.1007/978-1-4419-6749-7_26.

Song, Y., M. Ma, and F. Veroustraete. 2010. Comparison and conversion of avhrr gimms and spot vegetation ndvi data in china. International Journal of Remote Sensing,31(9), 2377–2392. doi: 10.1080/01431160903002409

Song, Y., and M.-G. Ma. 2007. "Study on VEGETATION Cover Change in Northwest China Based on SPOT VEGETATION Data." *Journal of Desert Research* 27: 89–93. 10.3321/j.issn:1000-694X.2007.01.021

Steven, M. D., T. J. Malthus, F. Baret, H. Xu, and M. J. Chopping. 2003. "Intercalibration of Vegetation Indices from Different Sensor Systems." *Remote Sensing of Environment* 88: 412–422. doi:10.1016/j.rse.2003.08.010.

Sun, J., X. Wang, A. Chen, Y. Ma, M. Cui, and S. Piao. 2011. "NDVI Indicated Characteristics of Vegetation Cover Change in China's Metropolises over the Last Three Decades." *Environmental Monitoring and Assessment* 179: 1–14. doi:10.1007/s10661-010-1715-x.

Sun, W., X. Song, X. Mu, P. Gao, F. Wang, and G. Zhao. 2015. "Spatiotemporal Vegetation Cover Variations Associated with Climate Change and Ecological Restoration in the Loess Plateau." *Agricultural and Forest Meteorology* 209: 87–99. doi:10.1016/j.agrformet.2015.05.002.

Sun, Y. 2012. "Variation of Vegetation Coverage and Its Relationship with Climate Change in North China from 1982 to 2006." *Ecology & Environmental Sciences* 21: 7–12. doi:10.3969/j.issn.1674-5906.2012.01.002.

Tian, F., M. Brandt, Y. Y. Liu, A. Verger, T. Tagesson, A. A. Diouf, K. Rasmussen, C. Mbow, Y. Wang, and R. Fensholt. 2016. "Remote Sensing of Vegetation Dynamics in Drylands: Evaluating Vegetation Optical Depth (VOD) Using AVHRR NDVI and In Situ Green Biomass Data over West African Sahel." *Remote Sensing of Environment* 177: 265–276. doi:10.1016/j.rse.2016.02.056.

Tian, F., R. Fensholt, J. Verbesselt, K. Grogan, S. Horion, and Y. Wang. 2015a. "Evaluating Temporal Consistency of Long-term Global NDVI Datasets for Trend Analysis." *Remote Sensing of Environment* 163: 326–340. doi:10.1016/j.rse.2015.03.031.

Tian, G. J., D. F. Zhuang, and M. L. Liu. 2003. "The Spatial-temporal Dynamic Change of Cultivated Land in China in 1990s." *Advance in Earth Sciences* 18 (1): 30–036. doi:10.11867/j.issn.1001-8166.2003.01.0030.

Tian, H., C. Cao, W. Chen, S. Bao, B. Yang, and R. B. Myneni. 2015b. "Response of Vegetation Activity Dynamic to Climatic Change and Ecological Restoration Programs in Inner Mongolia from 2000 to 2012." *Ecological Engineering* 82 (4): 276–289. doi:10.1016/j.ecoleng.2015.04.098.

Tucker, C. J., J. E. Pinzon, M. E. Brown, D. A. Slayback, E. W. Pak, R. Mahoney, E. F. Vermote, and N. El Saleous. 2005. "An Extended AVHRR 8-km NDVI Dataset Compatible with MODIS and SPOT Vegetation NDVI Data." *International Journal of Remote Sensing* 26: 4485–4498. doi:10.1080/01431160500168686.

Tucker, C. M. 1979. "A Reconnaissance Survey on the Quaternary History of St. Pierre Et Miquelon, France." *Maritime Sediments* 15: 27–34. doi:10.4138/1351.

Wang, G., and L. Han. 2012. "The Vegetation NDVI Variation Trend in Qinghai-Tibet Plateau and Its Response to Climate Change." In *Remote Sensing, Environment and Transportation Engineering (RSETE), 2012 2nd International Conference On. IEEE, 2012*, 1–4. doi:10.1109/RSETE.2012.6260792.

Wang, L., F. Tian, Y. Wang, Z. Wu, G. Schurgers, and R. Fensholt. 2018. "Acceleration of Global Vegetation Greenup from Combined Effects of Climate Change and Human Land Management." *Global Change Biology* 24: 5484–5499. doi:10.1111/gcb.14369.

Wang, S., X. Mo, Z. Liu, M. H. A. Baig, and W. Chi. 2017. "Understanding Long-term (1982–2013) Patterns and Trends in Winter Wheat Spring Green-up Date over the North China Plain." *International Journal of Applied Earth Observation and Geoinformation* 57: 235–244. doi:10.1016/j.jag.2017.01.008.

Wardlow, B., S. Egbert, and J. Kastens. 2007. "Analysis of Time-series MODIS 250 M Vegetation Index Data for Crop Classification in the U.S. Central Great Plains." *Remote Sensing of Environment* 108: 290–310. doi:10.1016/j.rse.2006.11.021.

Wenhua, L. 2004. "Degradation and Restoration of Forest Ecosystems in China." *Forest Ecology and Management* 201 (1): 33–41. doi:10.1016/j.foreco.2004.06.010.

Wu, D., X. Zhao, S. Liang, T. Zhou, K. Huang, B. Tang, and W. Zhao. 2015. "Time-lag Effects of Global Vegetation Responses to Climate Change." *Global Change Biology* 21: 3520–3531. doi:10.1111/gcb.12945.

Xiao, J., and A. Moody. 2004. "Trends in Vegetation Activity and Their Climatic Correlates: China 1982 to 1998." *International Journal of Remote Sensing* 25: 5669–5689. doi:10.1080/01431160410001735094.

Xin, Z., J. Xu, and W. Zheng. 2008. "Spatiotemporal Variations of Vegetation Cover on the Chinese Loess Plateau (1981–2006): Impacts of Climate Changes and Human Activities." *Science in China Series D: Earth Sciences* 51: 67–78. doi:10.1007/s11430-007-0137-2.

Xu, G., J. Zhang, P. Li, Z. Li, K. Lu, X. Wang and B. Wang. 2018. "Vegetation Restoration Projects and Their Influence on Runoff and Sediment in China." *Ecological Indicators* 95: 233–241. doi:10.1016/j.ecolind.2018.07.047.

Xu, X., J. Liu, Z. Zhang, W. Zhou, S. Zhang, R. Li, C. Yan, S. Wu, and X. Shi. 2017. "China's 5-year Interval Terrestrial Ecosystem Spatial Distribution Data Set (1990–2010) Content and Research and Development." *Journal of Global Change Data* 1 (1): 52–59. doi:10.3974/geodp.2017.01.08.

Xu, X., S. Piao, X. Wang, A. Chen, P. Ciais, and R. B. Myneni. 2012. "Spatio-temporal Patterns of the Area Experiencing Negative Vegetation Growth Anomalies in China over the Last Three Decades." *Environmental Research Letters* 7: 035701. doi:10.1088/1748-9326/7/3/035701.

Yu, F., K. P. Price, J. Ellis, and P. Shi. 2003. "Response of Seasonal Vegetation Development to Climatic Variations in Eastern Central Asia." *Remote Sensing of Environment* 87: 42–54. doi:10.1016/s0034-4257(03)00144-5.

Yun-Hao, C., L. Xiao-Bing, and X. Feng. 2001. "NDVI Changes in China between 1989 and 1999 Using Change Vector Analysis Based on Time Series Data." *Journal of Geographical Sciences,11* 11 (4): 383–392. doi:10.1007/BF02837965.

Zhang, B., C. He, M. Burnham, and L. Zhang. 2016. "Evaluating the Coupling Effects of Climate Aridity and Vegetation Restoration on Soil Erosion over the Loess Plateau in China." *Science of the Total Environment* 539: 436–449. doi:10.1016/j.scitotenv.2015.08.132.

Zhang, L., H. Guo, L. Lei, and D. Yan. 2011. "Monitoring Vegetation Greenness Variations in Qinghai-Tibet Plateau with MODIS Vegetation Index." *Geoscience and Remote Sensing Symposium (IGARSS), IEEE International. IEEE* 760–762. doi:10.1109/IGARSS.2011.6049241.

Zhang, Y., C. Song, L. E. Band, G. Sun, and J. Li. 2017. "Reanalysis of Global Terrestrial Vegetation Trends from MODIS Products: Browning or Greening?" *Remote Sensing of Environment* 191: 145–155. doi:10.1016/j.rse.2016.12.018.

Zhao, J., J. L. Liu, and L. Yang. 2012. "A Preliminary Study on Mechanism of LAI Inversion Saturation." *International Archives of the Photogrammetry, Remote Sensing and Spatial Information Sciences* 39: B1. doi:10.5194/isprsarchives-XXXIX-B1-77-2012.

Zhou, L., C. J. Tucker, R. K. Kaufmann, D. Slayback, N. V. Shabanov, and R. B. Myneni. 2001. "Variations in Northern Vegetation Activity Inferred from Satellite Data of Vegetation Index during 1981 to 1999." *Journal of Geophysical Research: Atmospheres* 106: 20069–20083. doi:10.1029/2000jd000115.